

Electrophysiological measurements of
spontaneous action potentials in crayfish nerve
in relation to the soliton model

Master's thesis

by

Rolf Justesen Pedersen

Membrane Biophysics Group,

Niels Bohr Institute,

University of Copenhagen

Supervisor: Thomas Heimburg

December 20, 2010

Contents

1	Introduction	1
2	Theory	3
2.1	The soliton model	3
2.1.1	Introduction	3
2.1.2	Requirements for soliton existence	3
2.1.3	The mathematics of solitons	4
2.2	Hodgkin on conduction velocity	6
3	Experimental methods and materials	7
3.1	A little biology of the Red claw crayfish	7
3.2	Electrophysiological measurements	7
3.2.1	Basic principles	7
3.2.2	Details of the setup	13
3.3	Data processing	16
4	Results and discussion	18
4.1	Introduction	18
4.1.1	Glossary and naming conventions	18
4.1.2	Peak classification using PAmpNAmp-plots	20
4.2	Prologue: Amplitude-speed correlation	24
4.3	Inherent uncertainty	26
4.4	Variation of parameters between experiments	26
4.4.1	Comparing widths in the primary and secondary channels	31
4.4.2	Peak width, local speed and average speed	34
4.4.3	Peak-to-peak time	35
4.5	Inter-dependence of the parameters	37
4.6	Temperature dependence of the parameters	38
4.6.1	Identifying corresponding peak classes between measure- ments	39
4.6.2	Comparing average peak profiles	41
4.6.3	Interpretation of amplitude and width results	45
4.6.4	Interpretation of speed results	47
4.6.5	Peak-to-peak times vs temperature	47
4.6.6	Recap of temperature dependence	48
5	Conclusions	52

Acknowledgements

Firstly I want to thank my supervisor Thomas Heimburg for inspiring talks about the theoretical background behind the project - and especially for a great deal of patience with my often obstinate ways, as well as for encouragement in spite of those.

I want to thank the members of the Membrane Biophysics Group at NBI for conversations in the lab (and elsewhere), and for always being willing to help me find my way around the equipment, both in locating it and in operating it - especially Andreas Blicher, Katrine Laub and Kasper Feld, with whom I spent most of the time in the lab.

With regards to helping out in the lab, a special thanks goes to Andreas Blicher, Ph.D student in our group, for taking a great deal of time out of his own project to help me out with all sorts of practical stuff in the lab - and not least of course, for writing, and continually customising and fine-tuning to my requests, the software routine that I used for data processing.

Thanks also to my friend Sara Ramskov-Andersen for providing me with the guide to thesis writing in LaTeX, that finally got me started writing. And to my father, Bent Pedersen, for conversations on nerve signals from a very different perspective.

Last but not least, a big thanks to Kristmundur Sigmundsson (Krissi) for essentially mentoring me with regards to lab work and biological knowledge, for the entire duration of our time in common at NBI. For spending a lot of his time teaching me the necessary knowledge, methods and tricks of the trade - especially with regards to all things biological - and for helping me gain some insight into what it is to be a researching scientist. And for 'coffee talks' at the local cafe about the pitfalls of scientific thought, as well as about completely non-scientific-related topics.

Abstract

The currently accepted model for signal conduction in nerve membranes, the Hodgkin-Huxley model from the 1950's, grew naturally out of a desire to explain the *electrical* phenomena related to nerves, because these were the ones easiest to measure at that time. Later, other phenomena of different natures were measured, and from a desire to explain these came a new proposal for the basic mechanism of nerve signal conduction, the soliton model, which is based on *mechanical and thermodynamical* grounds.

In this master's thesis I want to investigate in what way results based on the *old* electrophysiological measurements, can be related to and interpreted with the *new* mechanical soliton model.

For this purpose I measure the spontaneous (not artificially stimulated) action potentials (pulses) from a small motor nerve in the abdomen of the Australian red claw crayfish, using differential recording of the extracellular potential. The nerve contains six individual neurons, the action potentials of which can be distinguished by their differing amplitudes. Due to their spontaneous nature, the pulses pass the measuring electrodes separately and can thus be detected individually. Because of that, and the high number of detected peaks in each measurement (a few hundred to a few thousand), the natural variance within each neuron, of several pulse parameters can be reliably determined and used to judge whether a given change correlated with, for instance a change in temperature, is statistically significant or not.

The four pulse parameters amplitude, peak width (a measure of duration), speed and peak-to-peak time (time delay between positive and negative extrema of the pulse) are investigated for temperature dependence, and the results are - where possible - interpreted in relation to the predictions of the soliton model.

Chapter 1

Introduction

Nerves are cells like any other cells. Well, not *exactly* like other cells. The shape is different. They still have a cell body, a nucleus inside as well as a membrane as their 'skin'. But they also have protrusions called dendrites and axons. It is along those that the nerve signals - the action potentials - are transmitted. The dendrites carries the signals from other cells towards the nerve's cell body, and the axon transmits the outgoing signal on to still other cells. It has long been known that the nerve membrane plays a central part in the conduction of signals within the nerve. But the exact nature of this part is still not entirely clear.

Since A. L. Hodgkin and A. F. Huxley in 1952 [4] presented a detailed mathematical model explaining the - then readily measurable - electric effects of the action potentials, in part by currents of ions through the nerve membrane, this model has been taken in as the standard model of action potential conduction. This Hodgkin-Huxley model explains the conduction of nerve signals by analogy with electrical circuits, and thus it only accounts for the electric effects. Since then several other phenomena, not described by the Hodgkin-Huxley model, have been measured. They include reversible heat changes, thickness changes of the nerve and forces from the nerve on its surroundings, all during passage of an action potential. These phenomena are of a mechanical or thermodynamical nature and not included in the Hodgkin-Huxley model.

In recent years an alternative model has been under development ([2] and [6]), in order to explain these phenomena by invoking the idea of a special kind of density pulse, called a soliton, traveling along the nerve membrane. This model relies on the special properties of the membrane when it is near its melting temperature. The membrane consists mainly of lipids, which can exist in one of two main states (plus a few intermediate states not relevant to this discussion): gel or fluid. At normal physiological conditions the membrane is above (in temperature, that is), but near the phase transition between the two states. The soliton pulse consists of a localized overdensity in the membrane matter, in which this matter has gone largely through the phase transition and is mainly in a gel state.

The Hodgkin-Huxley model is, from a theoretical viewpoint, based on electrical analogies, and experimentally seen it was based on the electrical measurements, which were the ones accessible to experimentalists at the time. The soliton model, on the other hand, was invoked in trying to explain certain

mechanical and thermodynamical phenomena, which had not been explored when the Hodgkin-Huxley model gained ground - either because the technology was not advanced enough yet, or because people were too busy exploring the known and readily available electrical methods.

As far as the relationship between theory and experiments go, the Hodgkin-Huxley model has been closely connected to electrical phenomena, whereas the soliton model has grown out of mechanical and thermodynamical soil.

So the question I want to explore with this thesis is: To what degree are the electrical measurements in accordance with the mechanical (soliton) model?

For this purpose I have recorded electrically the action potentials from a nerve in situ, in the tail of specimens of the Australian red claw crayfish. I have measured the spontaneously occurring signals, in part because I assume them to be more like the signals in the living animal than the stimulated signals that are often measured on instead; but mainly in order to separate the signals from the individual neurons in the nerve, such that they can be analysed separately. I have recorded a large number of individual pulses from each neuron in each measurement, in order to get a statistically reliable measure of the inherent variance of the parameters characterizing the pulses, to be able to judge whether a specific change, especially between different temperatures, is statistically significant or not.

Where relevant and possible, I have compared the results with the predictions of the soliton model.

Chapter 2

Theory

2.1 The soliton model

2.1.1 Introduction

The soliton model is a description of special density pulses called solitons, as the basic underlying mechanism of the action potentials in nerves.

The theory is based on thermodynamics and was invoked by Thomas Heimburg and Andrew D. Jackson in 2005 [2] as an attempt to provide a theory that could explain the reversible phenomena and mechanical changes in nerves, described in the literature. *References here*

It describes these phenomena by taking into account thermodynamical concepts like heat and entropy, which are not a part of the currently accepted model for nerve pulses, the Hodgkin-Huxley model.

A soliton is a certain kind of sound pulse, special in that it does not dissipate its energy. Furthermore it does not change shape as it travels, and it is solitonic (i.e. localized).

Biological membranes - at temperatures just below the normal (body) temperature - often exhibit a phase transition between a gel-like state at lower temperatures and a fluid state at higher ones. A solitonic density wave can be said to consist of a gel-state portion of the neuronal membrane, moving along it, through the otherwise fluid-state membrane. It is thus not simply a propagating packet of overdensity - but also one that brings a local phase transition with it. It is this phase transition that makes the existence of solitons in lipid membranes possible.

2.1.2 Requirements for soliton existence

There are two formal requirements for the existence of a solitonic pulse:

1. non-linear dependence of the elastic constants on the density
2. dispersion - i.e. frequency-dependent sound velocity

Both of these requirements are demonstrated in figure 2.1, which shows data for a lipid membrane consisting of DPPC lipids (dipalmitoyl-phosphatidylcholine),

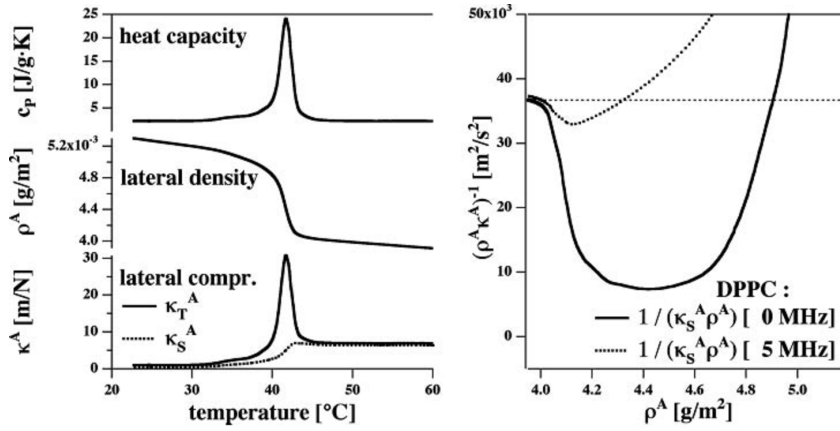


Figure 2.1: Data for a lipid membrane consisting of DPPC lipids, demonstrating the requirements for the existence of solitons. The right panel shows the sound velocity $c^2 = (\rho^A \kappa_S^A)^{-1}$ as a function of lateral membrane density ρ^A , for two different sound frequencies. That the curves are different shows that there is dispersion (frequency-dependent sound velocity). Furthermore, the non-linearity of the elastic constants κ_S^A and κ_T^A , can be seen in the bottom part of the left panel.

a lipid type common in membranes. The requirements are likely fulfilled near the gel-fluid phase transition.

The non-linearity of the elastic constants are shown in the bottom part of the left panel. The elastic constants are the isothermal and adiabatic area compressibilities, κ_T^A and κ_S^A respectively. They are measures of how much a specific area of the membrane changes in response to a small pressure change - at either constant temperature T (isothermal, κ_T^A) or constant entropy S (adiabatic, κ_S^A). The isothermal condition corresponds to a low-frequency case, the adiabatic to a high-frequency one. The difference between such two, for an extreme high-frequency of 5 MHz, is seen in the right panel of figure 2.1, showing the sound velocity $c^2 = (\rho^A \kappa_S^A)^{-1}$ as a function of lateral membrane density ρ^A , and indicating the second requirement: frequency dependence of the sound velocity. The lateral density ρ^A is the density of membrane matter measured per unit of length of the neuron. Its unit of mass per area comes about since a section of unit length, of the hollow-tube-shaped neuronal membrane, has a certain area (which for unit length is equal to the circumference of the neuron).

The frequency dependence of the sound velocity was established for DPPC membranes in the frequency range 1.3 to 13 MHz in [7]. It must be noted that this range is above the one typical for action potentials, which usually have durations of a few milliseconds, corresponding to frequencies below 1 MHz.

2.1.3 The mathematics of solitons

The general idea in the deduction of the equation describing the solitonic density pulses, is:

1. Take a basic differential equation for sound propagation, then
2. Substitute for the sound velocity factor c^2 an expansion to the second order in the lateral density ρ^A . This step incorporates the non-linearity.
3. Add a term that gives rise to dispersion (i.e. frequency-dependent velocity c).

plus a few other mathematical twists along the way.

If the membrane is approximated by a narrow cylinder the problem can be described as a propagation in 1 dimension, x , which then is the axis along the neuron cylinder.

The basic equation for sound propagation (without dispersion) is then:

$$\frac{\partial^2}{\partial t^2} \Delta \rho^A = \frac{\partial}{\partial x} \left(\frac{1}{\kappa_S^A \rho^A} \left(\frac{\partial}{\partial x} \Delta \rho^A \right) \right) \quad (2.1)$$

where $\Delta \rho^A = \rho^A - \rho_0^A$ is the difference between the lateral density ρ^A of the membrane, and the same at equilibrium (when there is no density pulse present), ρ_0^A . $\Delta \rho^A$ is a function of x and t , where t is the time. The $\frac{1}{\kappa_S^A \rho^A}$ is the sound velocity squared, c^2 . The non-linearity requirement is now incorporated by substituting c^2 with a non-linear expansion of it in $\Delta \rho^A$, of the form:

$$c^2 = \frac{1}{\rho^A \kappa_S^A} = c_0^2 + p \Delta \rho^A + q (\Delta \rho^A)^2 + \dots \quad (2.2)$$

The parameters p and q can be chosen to make the expansion fit data such as that from figure 2.1, left panel, as much as possible.

Furthermore, x and t are transformed together into the position coordinate $z = x - vt$, a coordinate in which the pulse is at rest, because it moves along with the pulse, both having velocity v .

A dispersive term $-h \cdot \partial^4 \Delta \rho^A / \partial z^4$ (where $h > 0$ is a free parameter connected to the length of the signal) is appended to the right-hand side of the equation. This gives rise to the other soliton requirement - the frequency-dependence of the sound velocity.

See [2] p. 9792 for more details.

The result is the differential equation describing the density pulse:

$$v^2 \frac{\partial^2}{\partial z^2} \Delta \rho^A = \frac{\partial}{\partial z} \left[\left(c_0^2 + p \Delta \rho^A + q (\Delta \rho^A)^2 \right) \frac{\partial}{\partial z} \Delta \rho^A \right] - h \frac{\partial^4}{\partial z^4} \Delta \rho^A \quad (2.3)$$

with v the velocity of the pulse.

This can be partly solved for $\Delta \rho^A$ to give:

$$h \left(\frac{\partial}{\partial z} \Delta \rho^A \right)^2 = (c_0^2 - v^2) (\Delta \rho^A)^2 + \frac{p}{3} (\Delta \rho^A)^3 + \frac{q}{6} (\Delta \rho^A)^4 \quad (2.4)$$

Equation 2.4 describes the soliton profiles seen in figure 2.2, for a DPPC membrane at $T=45^\circ\text{C}$ (left panel) and for lung surfactant at $T=37^\circ\text{C}$ (right panel). The profiles with higher amplitudes have lower velocities. Below a certain minimum velocity, $v_{min} = c_0^2 - p^2/6q$, solitons cannot exist. The soliton profiles with minimum velocity are the ones with the maximum amplitude, which is $\Delta \rho_{max}^A = |p|/q$.

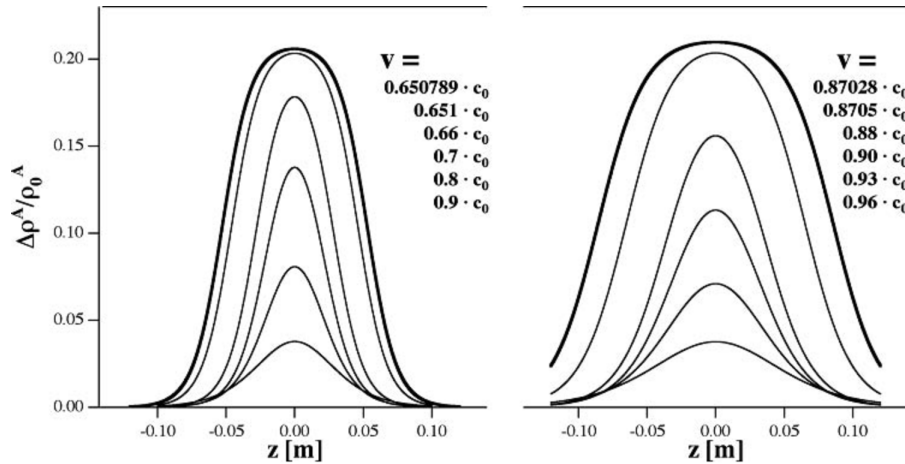


Figure 2.2: Soliton profiles for different velocities. Solitons with higher amplitudes have lower velocities. The upper curve in each panel represents the profile with the highest possible amplitude, and thus lowest possible speed. The left panel is for DPPC membranes at $T=45^\circ\text{C}$, the right panel is for lung surfactant at $T=37^\circ\text{C}$. The figure is from [2].

2.2 Hodgkin on conduction velocity

Hodgkin's 1954 article [3] gives theoretical arguments for the conduction velocity θ of the action potential along a non-myelinated axon being proportional to the square-root of the axon diameter d . He does give the following proviso, though: "*In practice, this relation is unlikely to be exactly obeyed since it is improbable that the membranes and axoplasm will be identical in fibres of different size.*" This is related to the fact that his conclusion depends on the specific properties of the membranes and the axoplasm being identical for different nerve fibres. The amplitude of the action potential is directly proportional to the axon diameter. Keynes and Aidley say about the amplitude: "*On theoretical grounds it might be expected to vary with the square of diameter, but Gasser's reconstructions provide some support for the view that in practice the relationship is more nearly a linear one.*" [5] (p. 19, first paragraph). It is not quite clear what the authors mean by 'Gasser's reconstructions' but I assume that they are referring to the book from 1937 by Erlanger and Gasser [1], since this seems to be their only reference including Gasser's name.

So we have for the conduction velocity θ , the amplitude A and the axon diameter d :

$$\theta \propto \sqrt{d} \quad (2.5)$$

and according to Gasser's reconstructions:

$$A \propto d \quad (2.6)$$

Together:

$$A \propto \theta^2 \quad (2.7)$$

Chapter 3

Experimental methods and materials

3.1 A little biology of the Red claw crayfish

Specimens of the Australian red claw crayfish (*Cherax quadricarinatus*), seen in figure 3.1, were used in the experiments in this project. Figure 3.2 shows a schematic of the animal seen from below, and a cross-section through the abdomen, approximately at the site of measurement. The severed abdomen, or tail, of a specimen, mounted in a tray during measurement, is seen in figure 3.3. The 'bridges' across the tail are called the sternum. They divide the tail into five equal segments. One of the bridges is cut away in this figure. The central nerve cord can just barely be seen running vertically, where the sternum is missing. In figure 3.4, which shows a colour-tainted view of one segment of the tail, the so called 'nerve 3', which is the nerve all measurements in this project are done on, is marked. It is the thin line running through the 'n'. The central nerve cord is the much thicker line running vertically.

The nerve 3 is a pure motor nerve, which means that all signals in it run exclusively from the central nerve cord out to the muscle at the outer end of the nerve. No signals go the other way. This is practical when one wants to measure the time delay between two electrodes on the nerve, of a signal, in order to find its speed.

The nerve contains a bundle of *six* axons, each from a different neuron. The six axons and their different diameters can be seen in the cross-section image of figure 3.5, where each axon is marked with an asterisk. The rest consists of glial cells and other facilitating cells.

3.2 Electrophysiological measurements

3.2.1 Basic principles

The idea of electrophysiological measurements on nerves or neurons is to detect the physiological action potential pulse electrically, with the use of electrodes. In this project I use differential electrodes to record the spontaneously occurring action potentials from a specific motor nerve in the abdomen of specimens of



Figure 3.1: The Australian red claw crayfish. Crayfish such as this one were used for the experiments.

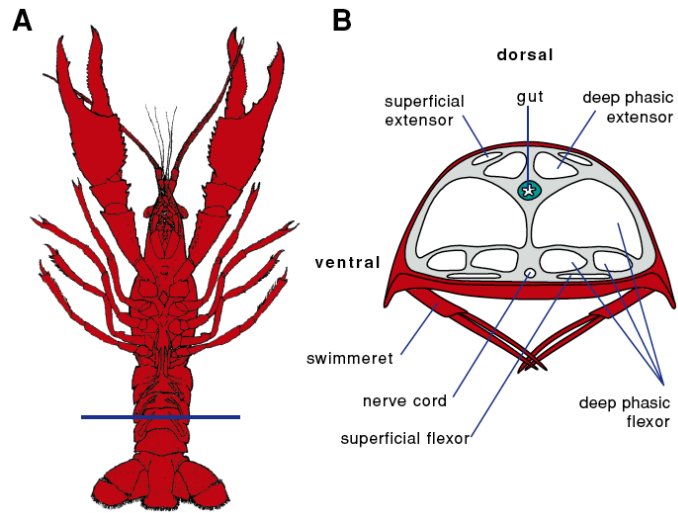


Figure 3.2: Schematic drawing of a red claw crayfish. Left part (A) is the animal as seen from below. Right part (B) is a cross-section from the blue line in (A). The nerve used to measure on extends from the central nerve cord in the middle out to the superficial flexor muscle, which it innervates.

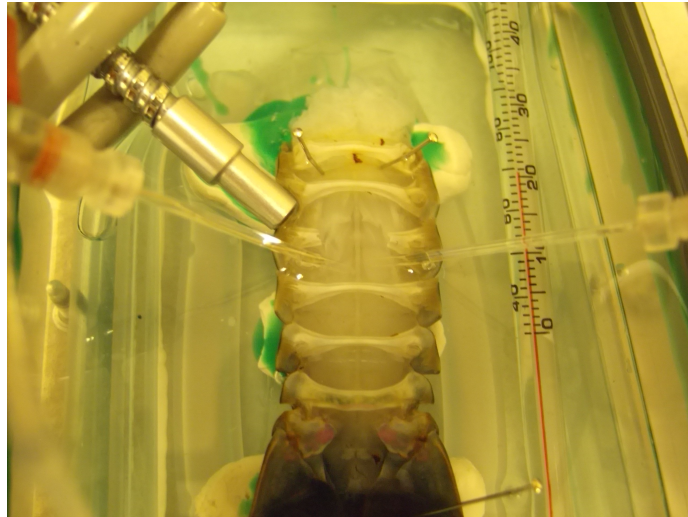


Figure 3.3: Crayfish abdomen, or tail, mounted and ready for measurement. The 'bridges' across the tail are the sternum, which divide the tail into five segments.

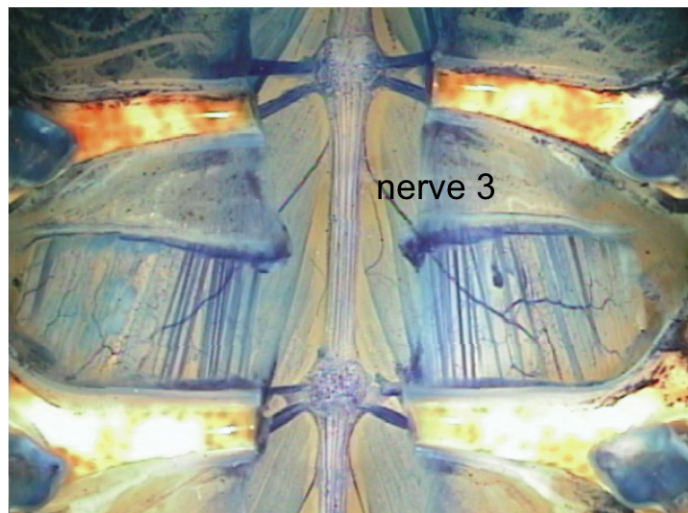


Figure 3.4: Colour tainted segment of a crayfish tail, showing the nerve used for measurements, nerve 3, as the thin line running through the 'n'.



Figure 3.5: Cross-section image of a nerve 3, featuring the six axons of different diameters that it contains, each marked with an asterisk.

the Australian red claw crayfish. Two electrodes are used to simultaneously measure the extracellular potential at two different positions of the nerve, a few mm apart.

The nerves transmit action potentials on their own, without the need for stimulation, for periods of sometimes up to 48 hours, even though the abdomen part of the crayfish was severed from the rest.

Differential recording

In my experimental setup I used differential recording of electrical potential from the crayfish nerves. In differential recordings the potential difference between two electrodes are measured by subtracting the potential measured by one electrode (the reference electrode, usually called -) from the potential measured by another (usually called +).

Not the standard method. A commonly used method to measure action potentials with differential recording is to place one electrode at one point of the nerve and its corresponding reference at another point further down the same nerve, in the direction in which the signal travels.¹ The object of this setup of course is to measure only the change in potential from a time when there is no action potential present, to when there is.

In my setup, on the other hand, this method was not used. I had the reference electrode placed several cm's away from the nerve² as can be seen in figure 3.6, which shows the specimen tray with a crayfish tail mounted in it. The tray is the rectangular box bounded by vertical gray plastic edges, its dimensions are 15×10 cm. The specimen was covered with a saline solution also containing a buffer. The saline was made to emulate the natural concentrations of salt ions in the extracellular fluid around the nerves.

¹Given that its a one-way nerve, i.e. that it only contains neurons in which the signals all move in the same direction.

²I tried once to use the aforementioned setup instead, but the result was the same, except for a rather larger noise level.

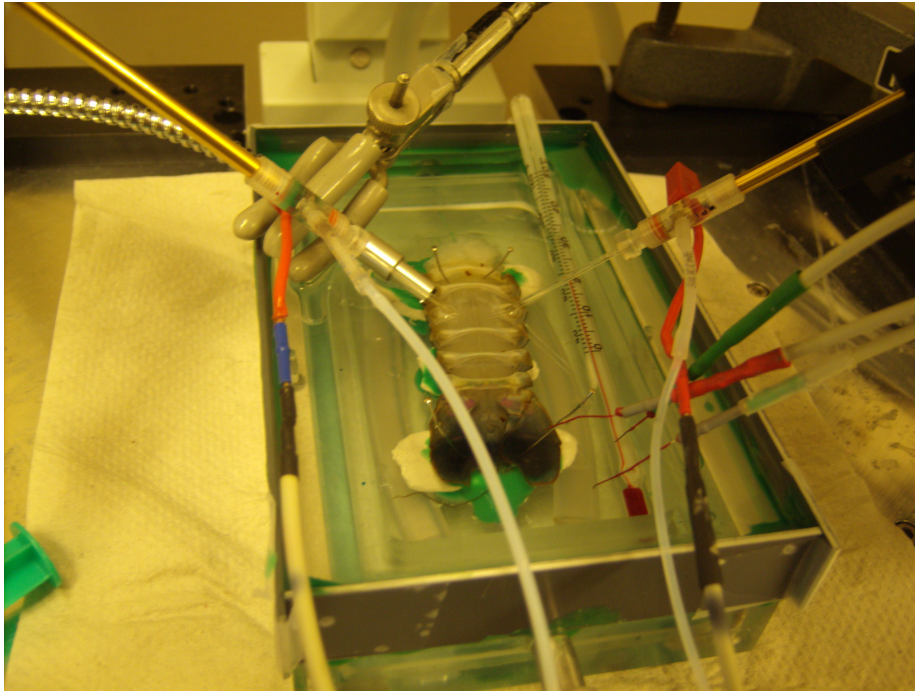


Figure 3.6: Specimen tray with crayfish tail. The tray is $\approx 15 \times 10$ cm. The tail, seen in the middle of the image is pinned to Blu-Tack on the tray's bottom with ordinary pins. The tail is covered with a saline solution emulating natural extracellular salt ion concentrations in the animal. Two glass capillaries containing the electrode wires can be seen attached to the middle part of the tail. Their reference electrodes, and the earth electrode, are placed in the saline solution in the lower right corner of the tray. The rippled metal wire to the far, upper left contains optical fibres that provide illumination of the specimen.

One of the two electrodes (+) measuring at the nerve is inside the glass capillary to the right of the tail (crossing the thermometer and ending at the crayfish abdomen). The reference electrode is one of the thin red wires in the bottom right part of the tray, near the lower end of the thermometer. The other two red wires seen near the bottom of the thermometer are: the reference for the other electrode in use; and the electrode connecting the saline solution to earth (through the amplifier). The wires are red because they have been painted with red nail polish for electrical isolation. The image shows the typical positions of the electrodes during measurements.

Suction clamping

As a means of attaching the electrodes to the nerve and keeping them at the same position, as well as to maintain a reasonably constant connection between electrode and nerve, suction clamping was used.

The suction clamping electrodes consist of a wire inside a glass capillary, the opening of which - at one end - has been made small enough to be on the same scale as the diameter of the nerve, which is on the order of $\approx 40\text{-}80 \mu\text{m}$. When

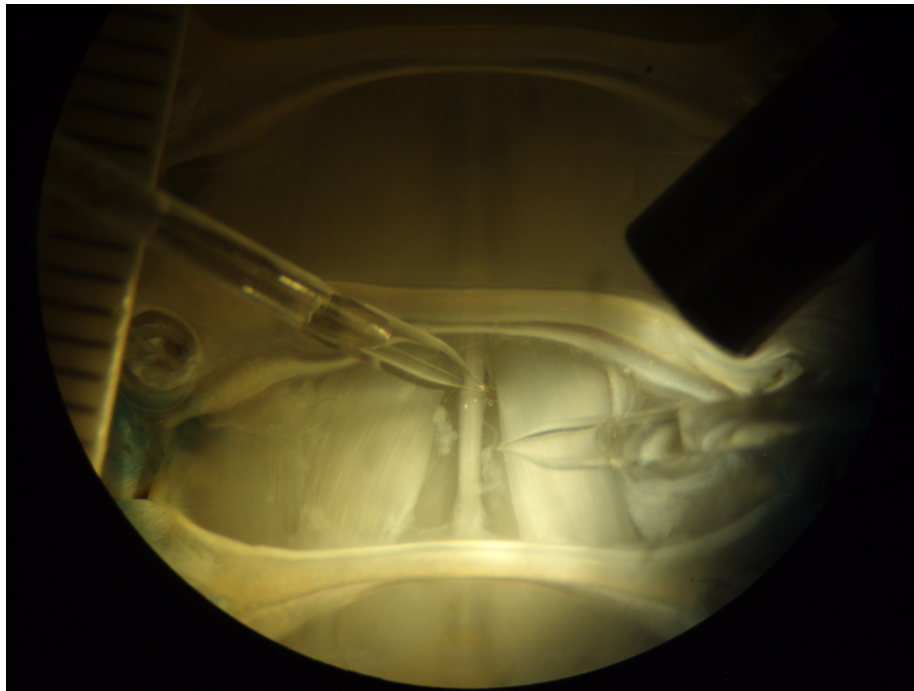


Figure 3.7: Two suction electrodes clamped on the same nerve, as seen through the microscope. The electrode wires are inside the glass capillaries that extend to either side of the image. The nerve whose signals are measured is a very thin, winding thread running between the pointed ends of the two capillaries, just to the right of the much thicker central nerve seen vertically in the middle. The outer diameter of the capillaries is 1.5 mm, the nerve itself is $\approx 40\text{-}80 \mu\text{m}$ thick.

suction is applied to the other end of the capillary, a small part of the nerve can be sucked into said small opening, ideally clogging it tightly and thus separating the volume inside the capillary from that on the outside. This ensures that the electrode only measures on the part of the nerve that is on the inside, and that it does not pick up noise through the saline solution.³ Figure 3.7 shows two electrodes (one glass capillary coming in from each side) clamped on the same nerve. The actual clamping happens at the narrow ends of the capillaries and cannot be seen at this magnification.

Two electrodes. The reason there are two electrodes measuring on the same nerve, is that in order to have a chance to measure the speed of the signals during a stretch of nerve, you need to detect the same signal at two different points of the nerve.

Extracellular recording. Furthermore, since the surfaces of the neurons are not penetrated by the electrodes, it is the potential at the extracellular side that is measured - relative to the potential in the saline solution far away, at the reference electrode.

³This also means that it, at any given time, only picks up the part of the signal that is currently inside the capillary.

3.2.2 Details of the setup

Electrodes, wires and glass capillaries

The suction electrodes I used each consisted of a piece of silver wire, chlorinated (i.e. coated with silver chloride, AgCl), and placed inside a glass capillary. The capillaries had an inner diameter of 0.84 mm and an outer of 1.5 mm (item no. 1B150F-3 from World Precision Instruments⁴).

Chlorination process. The chlorination of the wires was performed by placing them in a strong KCl solution of approximately 3M concentration, together with another silver wire to play anode when the first was cathode, and vice versa. The two wires were connected to the output of an amplifier (the same one I used for amplification of the nerve recordings, see below for details), one wire to the positive pole and the other to the negative. The output voltage of the amplifier was then controlled automatically from a computer, according to a predefined macro, using a software application called 'Scope', from AD Instruments⁵. The macro reversed the polarity of the two wires in the KCl solution several times during the process, taking a total of about nine to ten minutes before completion.

Capillary polishing. One end of the glass capillaries were made smaller in order to make the sizes of their openings comparable to the nerve diameter. This was done in three steps. First the capillary was pulled in two by heating and stretching it thin in the middle part, using a puller machine (model PC-10, from Narishige (Japan)). The stretching contracts the opening until it shuts. Secondly I cut off the tip of one of the parts with a scalpel, thereby opening a small hole in the end. Thirdly I polished this opening by holding it inside a flame for a few seconds. This melts the glass, and when it solidifies again the edges around the opening have changed from sharp, shattered glass to round and smooth and - provided good timing with the flame polishing - without melting the opening shut again.

A note on wire length. The length of the Ag/AgCl wires were approximately between 1 and 5 cm. The one which I call ch.3 (because it was connected to the channel 3 input on the amplifier) had the shorter wire length of ≈ 1.4 cm, while the other one, called ch.4 for obvious reasons, was $\approx 4 \pm 0.5$ cm.⁶ The inner ≈ 0.5 -1.0 cm of each wire was not chlorinated.

Holders and manipulators. The electrode silver wires were part of the microelectrode holders (order no. MEH7W) from World Precision Instruments, seen in figure 3.6 at the lower ends of the golden metal rods. Each holder had an outlet to which a 5 mL syringe was attached via a rubber tube (the pressure port on the holder to which the tube was attached, had an outer diameter of 2.0 mm). The syringes were used for applying suction through the capillary, thus enabling suction clamping of the nerve. Movement of the electrode holders was controlled through two micromanipulators. Initially in the experiment phase two manipulators from Narishige (Japan), both model NMN-25, was used. Later on one of them (the one used for ch.3) was exchanged for a model from Leitz (Germany) (model no. unknown). The syringes and micromanipulators are shown in figure 3.8.

⁴www.wpiinc.com

⁵from www.adinstruments.com

⁶Initially both were of the same length, but one of them broke in two, at some point during the experiments. Since this had no effect on the measured signals I saw no reason to replace it.

Reference electrodes

Each reference electrode was made of a small connector (≈ 1 cm long) which at one end could be connected to a wire from the amplifier. Into the other end was placed a piece of silver wire, which was then soldered to the connector. The wire was from Alfa Aesar⁷ (product no. 11468), its thickness was 0.25 mm and its purity 99.9985%.

A small piece of plastic tubing⁸ was then pulled in place around the connector, mainly to isolate it and thus preventing it from later getting into contact with the saline solution. The tubing was melted briefly (using the flame from a common disposable lighter), making it contract to fit tightly around the connector. Then most of the exposed silver part of the wire was painted with red nail polish to isolate it electrically. The outermost part, maybe around half a cm long, was left unpainted and was subsequently chlorinated using the same procedure as for the electrodes in the glass capillaries (see above section on that).

Specimen tray and water bath

A homemade specimen tray of dimensions 15×10 cm was used to place the crayfish tail in. The tray was made by Kristmundur Sigmundsson during his time as a Postdoc in the Membrane Biophysics Group at the Niels Bohr Institute. The tail was fixed to the bottom of the tray using (an imitation of) ordinary Blu-Tack as well as a two-component self-curing rubber replica (Reprorubber, reorder no. 16135, from Flexbar, NY, USA⁹) and ordinary pins (two through the first segment, two through the tail fins).

Subsequently the tray was filled with a saline solution, also functioning as a buffer, until the solution covered the nerve. This was done in part to emulate the natural extracellular salt ion concentrations in the animal (as mentioned above); and in part to keep the nerve and tissue etc. from falling on top of each other. If the organic material of the crayfish's insides are not kept in fluid, it makes it much more difficult to see what you are doing, when trying to clamp the electrodes onto the nerve. If they on the other hand are kept afloat in a liquid, they can more easily be moved around (using, for instance, a small glass poker).

The tray had hollow walls through which a temperature-controlled liquid, supplied from a water bath (ThermoMetric 5510 Thermostat (backside says 'Type LTD6G'), from Thermometric AB Sweden), could flow, in turn changing the temperature of the saline and subsequently also that of the nerve.

The temperature was measured with an ordinary thermometer (the one seen in fig. 3.6 placed in the saline solution).

A note on temperature equilibration times. I have to assume that the time it took for the nerve itself to equilibrate its temperature with the surrounding saline (or rather, with the part of the saline in the immediate surrounding of the thermometer) was negligible compared to typical times in the setup. For example, when cooling the saline, if the nerve equilibrates very slowly with the saline, then I might be measuring its signals at a higher temperature than what the thermometer shows. This is the case if it takes considerably longer for the

⁷www.alfa.com

⁸seen as the grey part of two of the electrodes in the lower right corner of the tray in figure 3.6

⁹www.flexbar.com

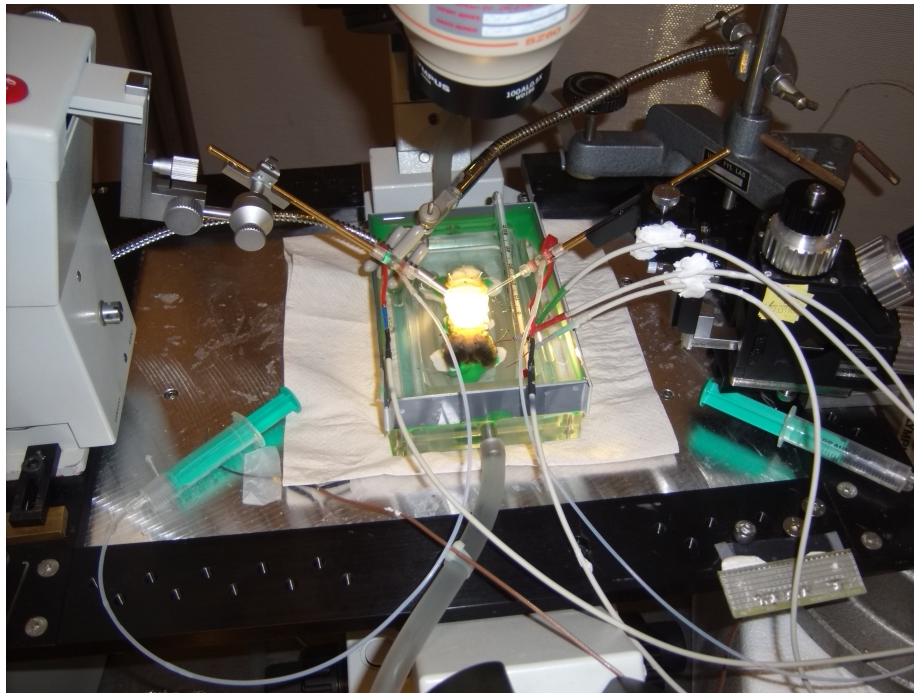


Figure 3.8: The setup for electrophysiological measurement, showing the two syringes (turquoise) used for suction, the tubing from and to the water bath, entering the upper and lower sides of the specimen tray, and the two (different) micromanipulators - one on each side - holding the electrodes. The 'snakelight', used for lighting the specimen, is visible on the left side behind the micromanipulator arm. The broad black frame marks the edges of the movable plate on which this equipment was mounted. Also, part of the top view microscope can be seen in the upper middle part of the image.

nerve to equilibrate, than it takes me to start the measurement, after I see that the thermometer shows the desired temperature - which is around half a minute to a whole. Even so, most measurements stretched over approximately ten minutes, and during almost all measurements the saline and nerve were equilibrating with the room temperature, because the water bath was turned off in order to remove the electrical noise it generated.

Lighting and microscope

Tray and micromanipulators were placed on a movable plate (see figure 3.8) mounted on top of an Olympus IX70 microscope¹⁰. What I will refer to as a 'snakelight' was used for illuminating the specimen. The snakelight is a flexible metal wire containing optical fibres. It is connected to a light source (model LQ 1600, from Fiberoptic-Heim, Switzerland), whose light is then led through the optical fibres to the end of the snakelight.

The specimen was observed through a stereo zoom microscope (Olympus SZ 60,

¹⁰which was not used to observe the specimen, since this microscope looks from below. The specimen had to be observed from above.

zoomfactor range 1 to 6.3) that was mounted so that it could be placed above the specimen.

Amplifier and data collection

The voltage picked up by the five electrodes - two were used for measuring at the nerve, two were used as their references, and one for connecting the saline to earth - was led to a PowerLab 26T amplifier from AD Instruments, using the cable (BioAmp cable, model Tronomed D-1540) that came with the amplifier. The connector on the BioAmp cable, where the five electrode wires are collected into one wire, is very sensitive to noise and had to be wrapped in aluminium foil.

The amplifier was connected to a computer, with which data was collected using the 'Chart' software from AD Instruments. Since it was necessary to resolve the individual peaks - which have a duration on the order of milliseconds - the amplifier's maximum possible frequency of data collection, 100 kHz, was used. That way the momentary voltages from the electrodes were recorded every 0.01 ms.

3.3 Data processing

The data recorded with the 'Chart' software was read into the 'Igor Pro' software from WaveMetrics¹¹, for data processing.

The data processing routine used for this project was written - and continually developed - by Andreas Blicher, Ph.D student in the Membrane Biophysics Group.

Basic peak detection. The two data channels from 'Chart', one for each recording electrode, were assigned to be primary channel and secondary channel for the data processing. The primary channel is the one used for the initial detection of peaks, therefore it is chosen to be the one with highest signal-to-noise ratio, since the detection is more reliable with a high signal-to-noise.

The routine then detects peaks in the primary data by setting a threshold voltage based on the baseline level and the background noise (the threshold can be fine-tuned by hand afterwards, if deemed necessary). Voltage maxima above this threshold are then identified as separate peaks.

Noise filtering. Prior to peak identification, the data processing routine allows for noise filtering using Fourier transformation of the data.

If the amplitude of the noise is larger than the amplitudes of the smaller peaks, this gives rise to problems with detecting these peaks without also falsely detecting each amplitude maximum in the noise as action potential peaks. This might then be prevented by Fourier transforming the original data to the frequency regime, then cutting out certain frequencies - usually those below 51 Hz and above 10000 Hz was cut - and Fourier transforming back to the time regime.

Only noise frequencies that are not too close to the frequencies of the actual peaks can be cut in this way without affecting the peaks themselves. The peaks have a duration on the order of \approx 1-5 ms, corresponding to frequencies in the range of \approx 1000 Hz down to 200 Hz.

Even so, the Fourier filtering has a tendency to produce 'tail flips' of the peaks, meaning that a curvature of the baseline close to the peaks tend to appear after

¹¹www.wavemetrics.com

filtering. For that reason Fourier filtering was only carried out when necessary to remove noise.

Peak detection in prim. and sec. channels. During the peak identification procedure the routine scans through the data, looking for a maximum in the voltage. Upon finding one it cuts out a predefined time interval (set by the user) around the peak maximum, and then starts looking in the secondary channel data, in that same time interval, for the nearest peak. This is almost always the correct corresponding peak, i.e. the very same action potential pulse, but detected a short while later in the secondary channel. This procedure is reliable because the time between consecutive peaks in the same channel is almost always several times larger (on the order of 0.1 s or more) than the delay time for one pulse between the channels - which is in the ms regime.

The routine does sometimes falsely detect artifacts caused by the other channel, giving rise to multiple detection of the same peaks. Details on that follow in section 4.1.2.

Some recorded parameters. The routine records the amplitudes of both positive and negative phases¹² as well as the peak widths, speed and several other parameters - for both the primary and the secondary channel.

The peak width - a width in time, and thus a measure for the duration of the pulse - was found at half the extremum of the voltage. This fraction was used in order to maximize the slope of the pulse shape at the points in time used to find the peak width. To determine peak width the routine must find out at what times the voltage rises above half the extremum value; and the higher the slope, the smaller the uncertainty in these times (due to the background noise the time determination is not exact).

The average speed between channels is calculated from a pulse's time delay between channels, together with the distance along the nerve between the electrodes.

The amplitudes, peak widths and speed - together with the time between positive and negative extrema, called the peak-to-peak time - are the main pulse parameters analysed in chapter 4.

¹²the *first* positive and negative phases, to be exact - since the pulses sometimes have secondary phases following the first ones, before settling back to the baseline.

Chapter 4

Results and discussion

4.1 Introduction

4.1.1 Glossary and naming conventions

In the following, **'experiment'** will mean a series of measurements, made at different temperatures, but all in one session. That is, all other parameters than the temperature was kept as constant as possible, including the two clampings of the nerve.

'Measurement' then will mean one continuous recording of voltage as a function of time, from both electrodes simultaneously. System temperature during a measurement changes somewhat due to equilibration with the surroundings (the water bath was kept turned off during measurements to prevent the huge noise in the measured voltages that it otherwise generated).

'Channel' (abbreviated ch.) means essentially the same as electrode, since each electrode was connected to its own channel in the amplifier. Due to numbering conventions used by the amplifier these are called channel 3 (or ch.3) and channel 4 (or ch.4).

The **'Primary channel'** is the channel selected, in the data processing software, for peak detection. This was always chosen to be the one with the highest signal-to-noise ratio, since this makes the peak detection more reliable and effective. **'Secondary channel'** is then simply the other one (subsequently peaks were also detected in the secondary channel, but with the occurrence times of primary ch. peaks as pointers of where to look).

'Upstream channel' means the electrode receiving each individual pulse first. It is the one clamped on the nerve closest to the central nerve cord, from where the pulses originate. All pulses travel along the nerve in only one direction (because it is a pure motor nerve), therefore each pulse is detected first in the upstream channel, and then a few milliseconds later in the **'downstream channel'** which is the one clamped further away from the central nerve cord, closer to the muscle where the nerve terminates. As a sidenote, the upstream channel is usually the primary channel, since upstream tends to have better signal-to-noise.

The names **'peak'**, **'pulse'** and **'signal'** are used interchangeably for the individual action potentials that were recorded from the neurons, so all three expressions mean the same thing.

'**Peak class**' is the result of the grouping together (classification) of certain peaks, primarily based on the similarity of their positive and negative amplitudes. Classification is always done using the primary channel data.

'**Positive amplitude**' means the amplitude (extremum of the voltage) of the first positive phase of a pulse. '**Negative amplitude**' then means the amplitude of the first negative phase.

Likewise then, '**positive width**' means the peak width of the first positive phase - and '**negative width**' means the peak width of the first negative phase.

If amplitude or peak width - or any other parameter that can be defined both for the positive phase and for the negative one - is mentioned without its 'sign' (positive or negative), then it can be assumed that it is for the *positive* phase.

'**Peak width**' means the full width of the pulse at half the maximum value of the voltage (half the amplitude). This is used as a measure of the width instead of the full width at the baseline, since the full width at half maximum is less subject to uncertainty caused by the background noise, than is the case for the width at the baseline (see section 3.3, subsection 'Some recorded parameters.').

'**Speed**' means the average speed between the two measuring electrodes, as calculated from the time delay between a signal being detected in the upstream electrode and the same signal being detected in the downstream electrode.

Peak classes are determined for each individual measurement and usually numbered according to the order of the approximate average of their positive amplitudes, from highest to lowest. So peak class number 1 normally has the highest amplitude, number 2 has the next-highest and so on. The classes are assigned numbers by the data processing routine in the order you add them as new classes, and they cannot readily be reordered afterwards, so in a few cases this numbering convention does not hold completely. But in these cases it is mostly because an outsider class with high amplitude, but only a few peaks, has been added as the last one.

The peak classes are named with a letter A or B signifying the channel in which their peaks have been detected, A meaning primary and B secondary ch. This is followed by their number according to amplitude. '**ClassA1**' would then be from the primary channel, and usually the one with highest amplitudes. Whereas '**classB3**' for instance would be from the secondary channel, and the one correlated with classA3 from the primary ch. A and B classes with the same number always consist of the same peaks, since each peak in the B class is the one closest in time to a specific peak in the same-numbered B class.¹

In the figures each peak class has a different colour. In a few cases the colours for corresponding classes do not match across figures, but in these cases it is pointed out in the text.

The naming conventions of the experiments/measurements are as follows. Each experiment is identified by a six-digit number coding the date the experiment was carried out. For example the series of measurements used for analysing temperature dependence is called 100203, because it was recorded on February 3rd 2010. Each individual measurement within an experiment is then furthermore numbered by a two-digit number in the order the measurements were recorded. For instance measurement number 2 from June 18th 2010 is called 100618.02. There may be omissions in these numberings, because some

¹the closest one is almost always the actual corresponding peak. Confusion of peaks occur very rarely because the time between consecutive peaks is several times larger than the delay of a peak from one channel to the other.

of the measurements were not used due to too much noise or lack of signals.

The general strategy of data analysis will be to use most of the 100203 measurement series to investigate temperature dependence of the pulse parameters, and the 100618_02 and 101007_08 measurements for external comparison, to get an impression of the variance between different experiments.

The pulse parameters, which are investigated, are:

- amplitude
- peak width
- speed
- peak-to-peak time

Amplitudes and peak widths are, unless otherwise noted, for the first positive phase of the pulse (i.e the one with positive voltages). Peak width is the full width (in time, i.e. a duration) of the pulse at half the maximum. Speed is the average speed of the signal between the two electrodes. Peak-to-peak time is the time that elapses from the pulse reaching its positive extremum to when it reaches its negative extremum.

Figure 4.1 shows an example of the average shape of pulses (action potentials), taken from the 100203_10 measurement. Each of the three coloured curves represents the average of a separate peak class, calculated from the individual peaks in that class. The data is from the primary, upstream channel, at 15°C. The profiles feature amplitudes of a few hundred μV and durations of a few ms, which are typical numbers.

Figure 4.2 shows the same three peak classes (from the same measurement) in the secondary, downstream channel. A larger noise is seen, as well as smaller amplitudes, below 100 μV , which is natural since it is selected for in the secondary channel. It also shows longer durations, which is not always the case for the secondary channel. This is discussed in further detail later.

As mentioned above the upstream channel has a tendency to higher signal-to-noise ratios than the downstream one. This could be because the nerve usually is thicker at that position, and that its diameter here generally fits the opening size of the electrodes' glass capillaries better. But the openings are hand-made and therefore have a more or less random distribution of sizes, not likely to be correlated with the position of the capillary on the nerve.

Instead, the shuffling around of the amplitudes of the peak classes in the downstream channel, as compared to the upstream, as well as the odd shapes of the peaks in the former (which is a general phenomenon not only present in figure 4.2) could be caused simply by the presence of the upstream channel being clamped on the nerve. The clamping itself could maybe exert some sort of stress on the neurons, thereby affecting their ability to transmit the signal unchanged.

4.1.2 Peak classification using PAmpNAmp-plots

PAmpNAmp is short for Positive Amplitude vs Negative Amplitude. Figure 4.3 shows such a plot, which is the main plot type I used for most classifications of the peaks.

Following standard procedure in the field of electrophysiological measurements

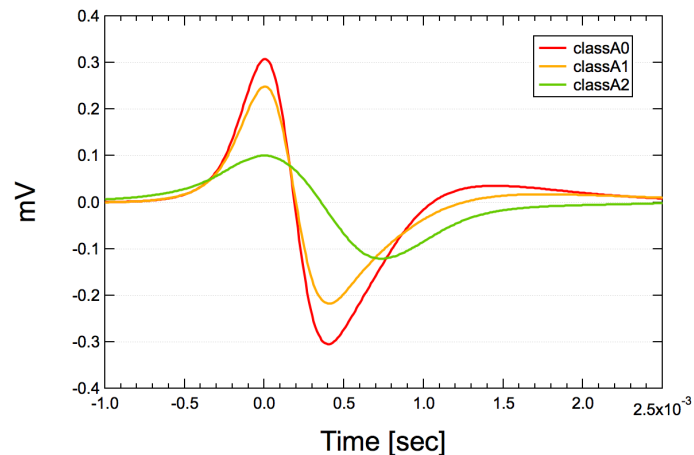


Figure 4.1: An example of peak shapes - from the primary, upstream channel. The figure shows profiles for the three peak classes detected in the 100203.10 measurement at 15°C. Each curve is calculated as the average of all the peaks in that class. Amplitudes and durations have values typical for the experiments.

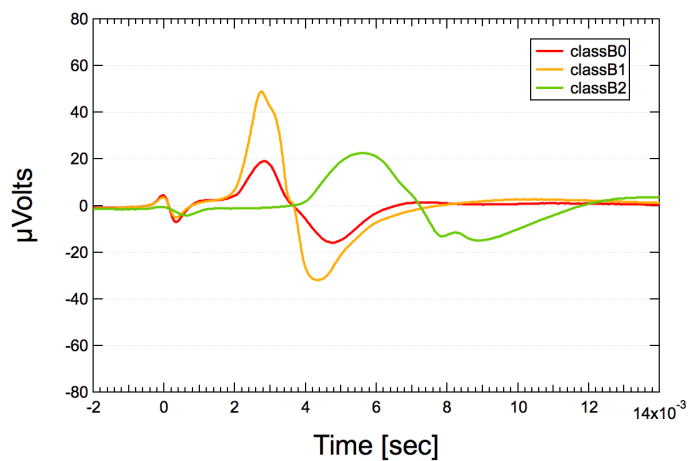


Figure 4.2: Average peak profiles for the same three classes as in fig. 4.1 - but from the secondary, downstream channel. It is seen that the order of peak classes with respect to amplitude is not conserved from the upstream to the downstream channel. The small signal at 0 ms is an artifact caused by the signal in the primary channel.

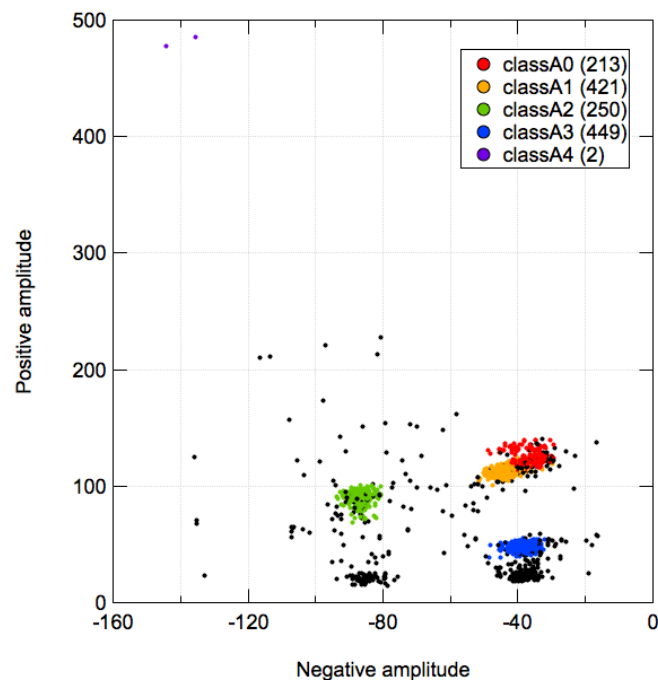


Figure 4.3: Plot of amplitude of the negative phase vs amplitude of the positive phase of the peaks. The classification of the peaks uses plots such as this one. Each data point represents an individual peak, colours represents classes, and black points are unclassified peaks. Numbers in parentheses in the legend are the number of peaks in each class. Amplitudes are in μV . Data is from the first 1 minute from the measurement 101007_08.

of action potentials, I primarily classified the peaks according to their positive and negative amplitudes, thereby assuming that each individual neuron has its own separate amplitude range, which is distinguishable from those of the other neurons in the nerve. The classification was done by inspection of the PampNAmp-plot, identifying localized clusters of data points and then classifying those into one peak class, assigning a different colour to each class, leaving the unclassified peaks as black data points.

The unclassified clusters below the green and blue classes are 'shadows' of those classes. The shadow classes consist of peaks that are detected twice due to small but significant bumps on either side of the actual maximum of the peak, bumps which the detection routine mistakes for separate peaks. See figure 4.4, where such a bump can be seen in the blue trace. The figure shows average profiles -

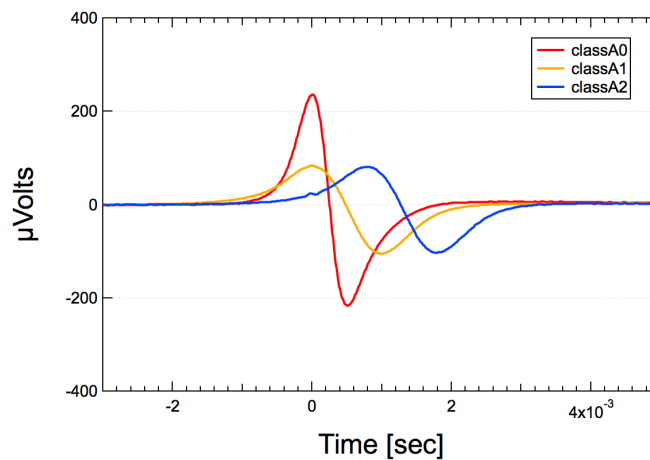


Figure 4.4: Average peak profiles for three classes that are in reality only two. From the 100203_09 measurement. Some of the peaks in the yellow class have been detected twice, because of a bump on the rising phase, seen in the blue trace. This gives rise to the 'shadow classes' with smaller positive amplitude, but the same negative amplitude, seen below the green and blue classes in fig. 4.3.

albeit from a different measurement and experiment than the one in figure 4.3 - for the detected peak classes in the 100203_09 measurement (at 5°C). The blue class is in reality included in the yellow class, and consists of such doubly detected peaks. The bump is probably caused by electronic crosstalk between the two recording channels, which is a phenomenon where a sufficiently large voltage in one channel also shows up in the other, as a much smaller voltage. This double detection explains why the shadow classes have the same negative amplitude as their 'parent' classes (here the green and blue); they simply have the same negative phase.

The data shown in figure 4.3 consists of peaks recorded during the first minute (out of a total of ten minutes) of the measurement 101007_08. Due to the lower number of pulses during this shorter interval, the peak classes are more distinct. At least in this particular experiment the spread of amplitudes becomes larger when using the pulses of, f.i., the first eight minutes instead, and this makes it harder to distinguish the separate classes by eye.

This PampNAmp-plot shows that there need not be a constant ratio between positive and negative amplitudes.

I will focus my attention on the positive phase of the pulses, because it has the most reliable correlations, whereas the negative phase often shows irregular behaviour, sometimes disappearing altogether during the same clamping.

This might be caused by changing temperature or by the acetylcholine chloride, that was sometimes added to increase firing frequency. In theory it should be the *negative* phase that corresponds to the actual action potential (see for instance [8], p. 57) , at least according to the standard model of nerve signal conduction, the Hodgkin-Huxley model. Following that, the potential on the outside of the nerve membrane - which is what I am measuring - should be more negative during the passage of an action potential pulse, than when there is no pulse present. This apparent polarity reversal might simply be due to miswiring somewhere in the setup, although I have checked the setup thoroughly for that. Based partly on this setup check, and partly on my observations of the positive phase being more reliable and stable than the negative one, I will from hereon assume that the actual signal is represented by the **positive** phase.

4.2 Prologue: Amplitude-speed correlation

Figure 4.5 shows positive amplitude as a function of signal speed, showing a positive correlation: peak classes with larger amplitudes also have higher speeds. The connection could be linear, especially if one ignores the purple peak class A4, which consists of only two peaks with very high amplitude near the top of the figure.

'Speed' - unless otherwise noted - means average speed between the channels, i.e. between the two electrodes measuring the signal. This speed is calculated from the signal's propagation time from the first electrode that detects it (called the upstream electrode) until detection by the second one (the downstream electrode). Taking into account the possibility that the speed of the signal is not constant when it is traveling along the neuron, the speed value calculated in this way is therefore technically an average speed for the stretch of nerve between the two electrodes.

The average speed is usually encumbered with some uncertainty, in part because it is not very easy to get a good measurement of the distance along the nerve, from the upstream electrode clamping site to the downstream one (see figure 3.7); and in part because of the rather short distances involved (on the order of 1 to 3 mm)², causing larger relative uncertainties.

Figure 4.5 shows a detection defect in the yellow peak class (A1). In this measurement the signals that were classified into class A1, using the primary channel data, were not detected at all in the secondary channel. Presumably this was because the positioning of the nerve in the secondary channel clamping prevented the signals from that particular neuron from being detected by the electrode.

This makes a calculation of the speed impossible. Instead the data processing routine simply finds the next peak in the secondary ch. data set, which then is located a more or less random amount of time after the occurrence of the original peak in the primary ch. This explains the low speeds and the large spread in class A1 (yellow) in figure 4.5.

²the total length of the nerve is only maybe 5 to 8 mm.

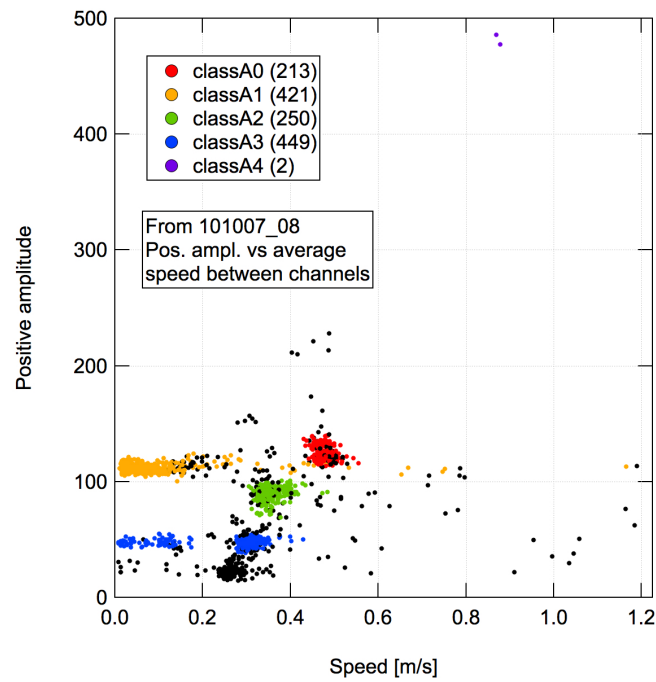


Figure 4.5: Positive amplitude vs speed for the same data as fig.4.3 (1 minute of measurement). It shows a positive correlation - classes with larger amplitude also have higher speeds. The data points for classA1 (yellow) should be disregarded in this plot, because a calculation of speeds for this class was not possible since its peaks were not detected in the secondary channel. The same is true for the part of classA3 (blue) with lower speeds. (Note the two purple peaks near the top.)

4.3 Inherent uncertainty

It is expected that some of the properties of the pulses change, when the temperature of the system changes. But in order to get a better knowledge about what part of this is actually caused by the altered temperature, we must also examine how the pulse properties depend on other factors, as well as on each other. Some of these other factors are inherent to the experimental setup and cannot be controlled. Others can be controlled to a certain limited degree, or can at least be observed to some precision.

The first thing to look for is the inherent random uncertainty in the pulse properties: how much do they change, when the external conditions are being kept as constant as possible. An example could be the spread in amplitude within one peak class in a given channel, without manipulating the clamping (that is: without unclamping the nerve, without moving either the nerve or the glass capillary, and without changing the strength of the suction).

Such uncertainties are quantified here as standard deviations, calculated from Gauss curves fitted to histograms of the pulse parameters.

4.4 Variation of parameters between experiments

Figure 4.6 shows plots of amplitude and widths of the positive phase of the peaks, as a function of signal speed. The data is from 100618.02, where the temperature was $\approx 15^\circ\text{C}$.

The upper panel (amplitude vs speed) can be compared with figure 4.7, which is a similar plot, at approximately the same temperature - but from a different experiment (100203.07).

Assuming:

- that each colour represents the same neuron in both plots
- and that each neuron always transmits signals with the same intrinsic amplitude, given constant temperature

and noting that the amplitudes in one plot are almost twice as large as in the other one, this then indicates that the measured amplitude varies between experiments. This is most likely due to differences in the clamping qualities. This of course makes it harder to identify, from their measured amplitudes, the individual neurons between different experiments.

As mentioned, the speeds differ between the two experiments, but since the speed is calculated from the distance along the nerve between the two measuring electrodes, and this distance has a quite large uncertainty to it, so has the speed. The electrode distance in the 100203.07 measurement was judged to be $3\text{ mm} \pm 0.5\text{ mm}$, so its relative uncertainty is $\approx 17\%$. For the 100618.02 measurement it is $\approx 11\%$ (distance was 2.0-2.5 mm). These uncertainties are almost enough to explain the speed discrepancies of each peak class, between the two experiments. But the uncertainties are themselves uncertain, because they had to be judged more or less arbitrarily with the naked eye. Therefore I judge it to be likely that the speeds do not vary significantly between experiments.

Figure 4.8 shows the positive peak width in the primary channel, as a function of the speed, for the 100203.07 measurement. Comparing this with the

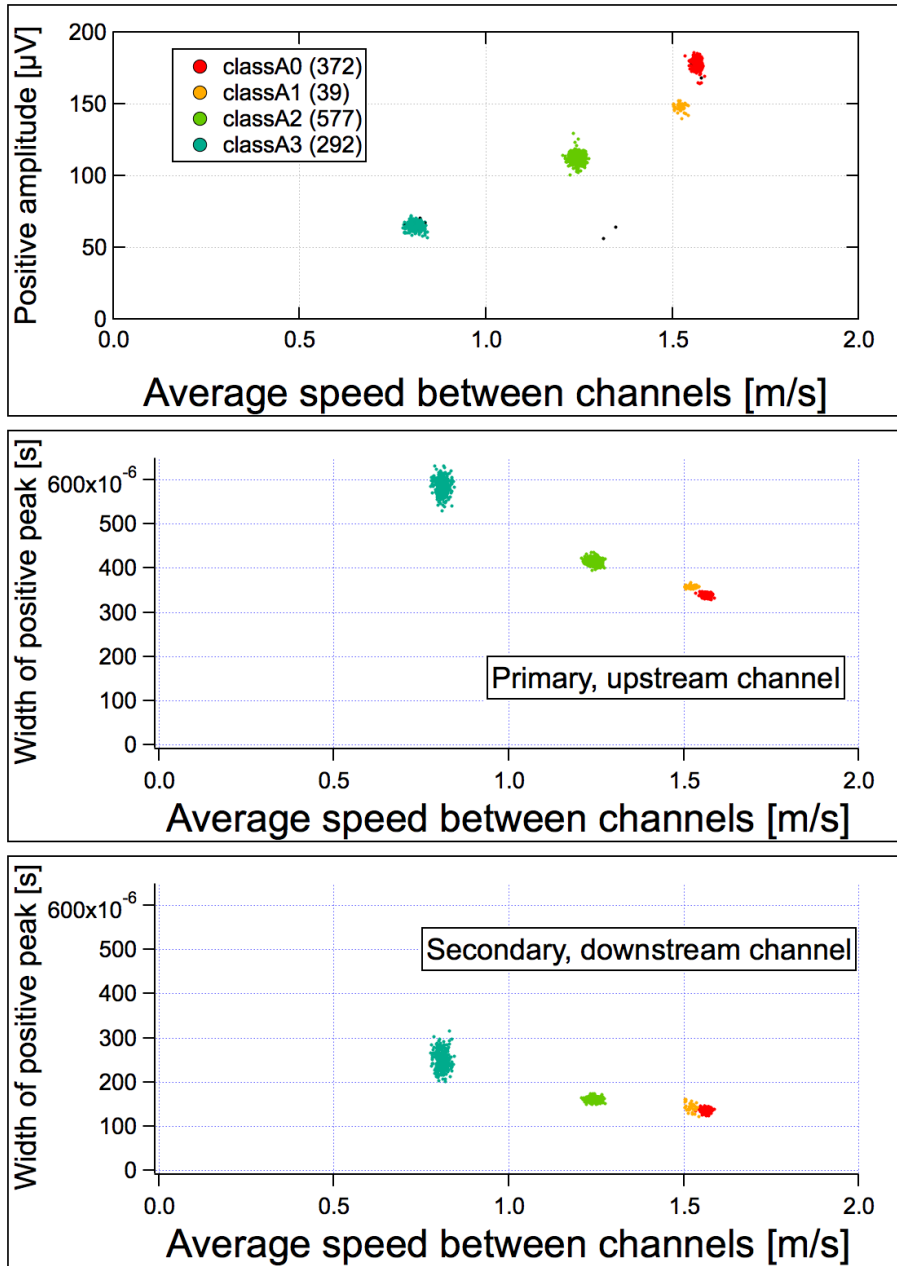


Figure 4.6: Plots of amplitude and widths as function of speed, for the positive peak. Experiment 100618_02. Upper panel: Amplitude vs speed. Middle panel: Width (in seconds) vs speed for the primary channel, which was located upstream during measurement. Lower panel: Width (in seconds) vs speed for secondary ch., located downstream. Numbers in parentheses in the upper panel denote the number of peaks in that class; class colouring is the same in all three panels. Temperature is 15°C . Units are denoted by square brackets.

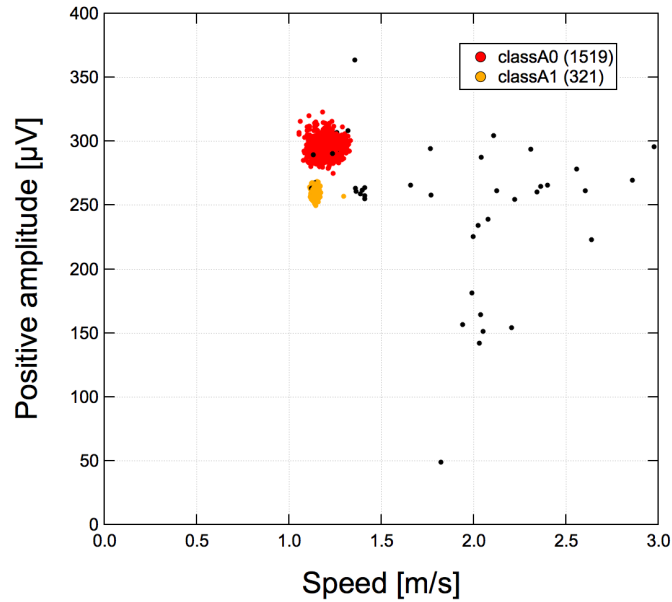


Figure 4.7: Positive peak amplitude as function of speed, from experiment 100203_07. Temperature is 15°C, numbers in parentheses denote the number of peaks in that class. Black points are unclassified peaks. Comparison with fig. 4.6, upper panel, shows somewhat different amplitudes, and slightly different speeds (equal, to within uncertainties).

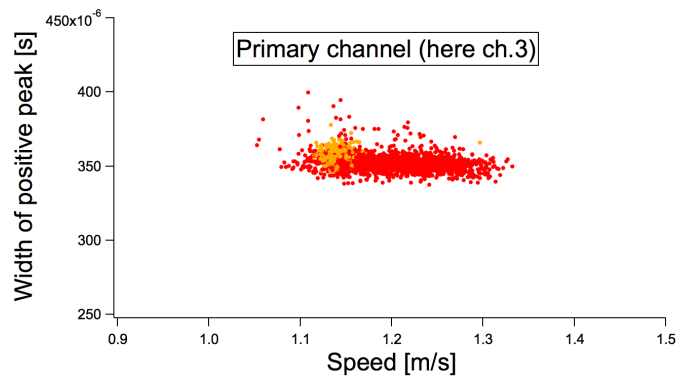


Figure 4.8: Positive peak width in the primary, upstream channel, as a function of speed. From experiment 100203_07. Red data points are classA0, yellow ones are classA1. Temperature is 15°C. Width values are comparable to those of classes A0 (red) and A1 (yellow) in fig. 4.6, middle panel, while speeds are different due to uncertainties in that parameter.

middle panel of figure 4.6 - assuming colours correspond to each other - it seems that, for each class, the widths are approximately the same in both plots. The average values and standard deviations (Stdv) of the peak widths are:

Peak width in 100618.02 measurement		
peak class (neuron)	Average [ms]	Stdv [ms]
classA0(red)	0.339	0.003
classA1 (yellow)	0.358	0.003
Peak width in 100203.07 measurement		
peak class (neuron)	Average [ms]	Stdv [ms]
classA0(red)	0.352	0.006
classA1 (yellow)	0.358	0.005

Comparing, for each table, the difference between the average values with the sum of the standard deviations, it is seen that classA1 has the same width, to within one Stdv, in both measurements, but the widths of the two classA0's differ by more than the sum of their Stdv's. This discrepancy is probably not caused by small differences in temperature then, since it is not the same for both classes.

The peak width depends on the local speed of the signal at the clamping site, so this difference between the two classes shows that the signal speed in a given neuron³ need not be the same in two different experiments. But if signal speed depends on the diameter of the neuron, then this of course could be explained by the two neurons - which are from two different crayfish specimens - simply not having the same diameter in both specimens.

Peak widths might seem rather unchanged in the primary channel, but when comparing the widths from the secondary channel a different picture emerges. Figure 4.9 shows width as function of speed for the secondary channel in the

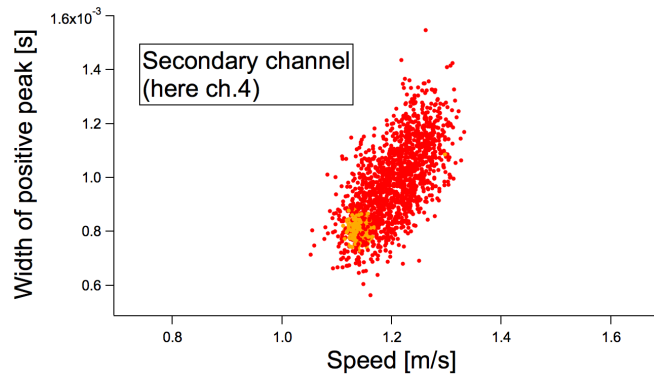


Figure 4.9: Positive peak width in the secondary, downstream channel, as a function of speed. From experiment 100203.07. Temperature is 15°C. Width values are larger than in fig. 4.6, lower panel.

100203.07 measurement. Note the scale on the width axis. No exact values of

³the term 'given neuron' not being entirely well-defined across experiments; it assumes implicitly that the six neurons have the same set of diameters in all crayfish specimens.

the average width is necessary to see that they differ quite a lot from those in the lower panel of figure 4.6. They are at least twice as large - more, if we still assume that the class numbers/colours correspond to each other across the two plots. This discrepancy could be due to detection uncertainty caused by the lower signal-to-noise ratio in the secondary channel.

The majority of the higher values in the red class must be due to a misdetection

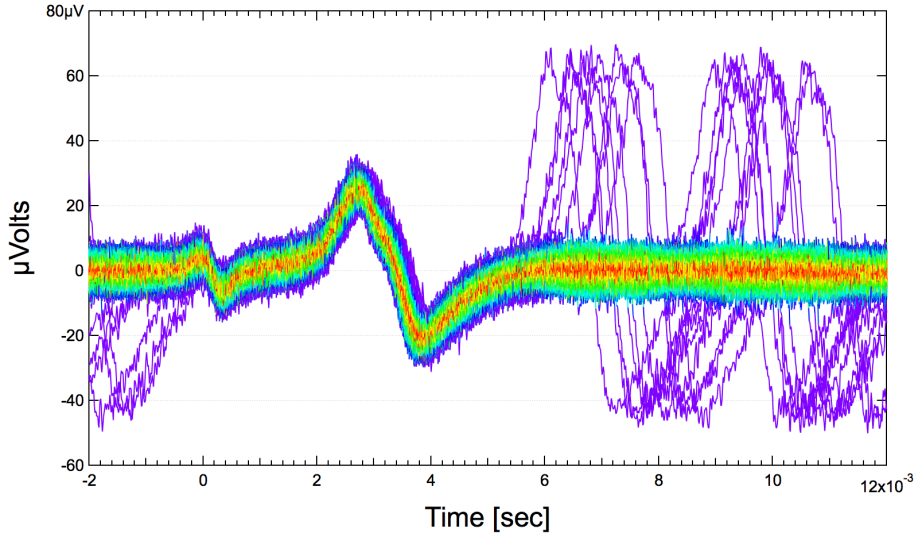


Figure 4.10: Plot of the 1519 peaks in the red classB0 from figure 4.9 (downstream channel), aligned so their positive peaks coincide. The colour-coding shows the deviations from the class average, from red meaning least deviation to purple meaning most. The high-amplitude purple peaks are nearby ones from the other class. The small peak at 0 ms is an artifact due to crosstalk between the channels. It is caused by the detection of the peak in the primary channel.

during data processing. In figure 4.10 the 1519 peaks in the red classB0 (downstream channel) are plotted on top of each other, colour-graded after how much they deviate from the class average - spanning from red for least deviation to purple for most. This gives an impression of the variance within the class. More importantly it shows that the peak, located at around 2-4 ms, is preceded by a slow rise between 0.5 and 2 ms before going into the actual peak, not present in figure 4.11, which shows an example of a typical peak shape. Due to this atypical, slow incline together with the high level of noise, the detection routine - looking for when the width values first rise above half the value at the top of the peak - detects crossing of that threshold at a considerably earlier time than it should. This most likely is the cause of the width values above ≈ 1.2 ms in the red class in figure 4.9. The 1.2 ms is the width (at half height) of the actual positive peak phase, as judged with the naked eye from figure 4.9. In both figure 4.10 and 4.11 a small peak is seen at 0 ms. This is an artifact caused when the same signal is detected in the primary, upstream channel. It is due to crosstalk between the channels - which is when one channel is affected by what is detected by the other.

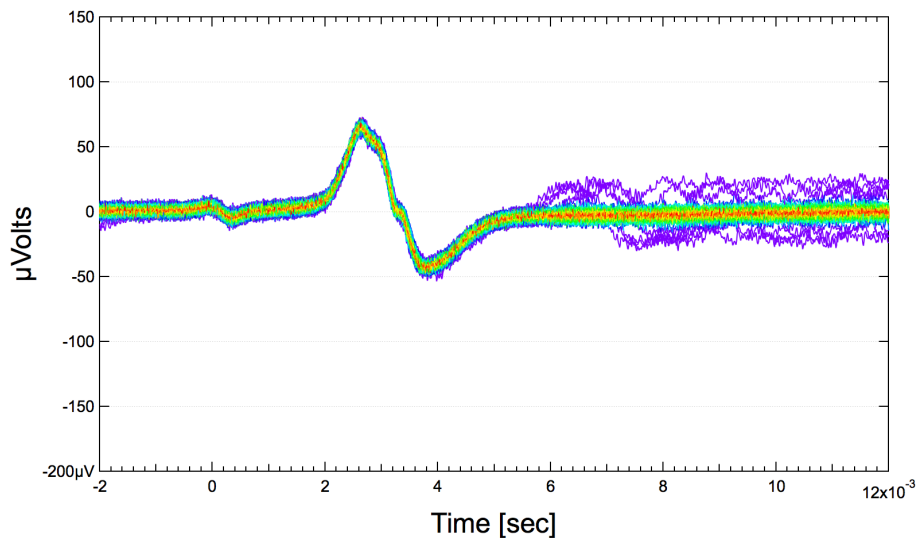


Figure 4.11: Plot of the 321 peaks in the yellow classB1 from figure 4.9, aligned so their positive peaks coincide. Again there is an artifact from inter-channel crosstalk at 0 ms (as in fig. 4.10).

To sum up, the positive amplitudes vary significantly between different experiments, making it difficult to identify corresponding peak classes across experiments.

On the other hand, it seems that the positive widths may be more constant - at least in the primary channel. The differing widths in the secondary channel might ultimately be caused by the lower signal-to-noise ratio inherent to that channel.

The speeds also might be comparable between experiments, to within their (quite large) uncertainties.

4.4.1 Comparing widths in the primary and secondary channels

From the middle and lower panels of figure 4.6, as well as from comparison of widths in figures 4.8 and 4.9, it is seen that there is a significant difference in peak widths between the primary and the secondary channels, a difference that is larger than the spread inherent to each channel. Figures 4.12 and 4.13 show direct comparisons for the 100618.02 and 100203.07 measurements, respectively. Since the primary channel is in both measurements also the upstream channel (i.e. the one detecting the signal first) it might look initially like the signal is decelerating from the upstream to the downstream ch. in one experiment (figure 4.13) and is accelerating from upstream to downstream in the other experiment (figure 4.12)⁴.

Here it is important to note that even though the primary channel is also the

⁴An accelerating signal might seem a little strange at first, but would in principle be possible if the axon diameter were to increase further down the nerve.

upstream channel in both measurements, the actual electrodes - named ch.3 and ch.4 - were interchanged. This means that in both cases the larger widths are measured by the same electrode - namely ch.4 - suggesting that the width increase is somehow connected to the electrode and not to the nerve itself, nor to the position of the electrode relative to the other (upstream or downstream)⁵. The only plausible explanation for this, that comes to mind, is the fact that the ch.4 electrode (at least for some experiments, maybe all of them - this knowledge was not recorded) had a shorter electrode wire, around one-third of the wire length in the ch.3 electrode. This might have caused generally larger peak widths to have been detected, in that it increased the duration in which the electrode wire was exposed to the signal in the nerve, because of a delay time from nerve to wire.

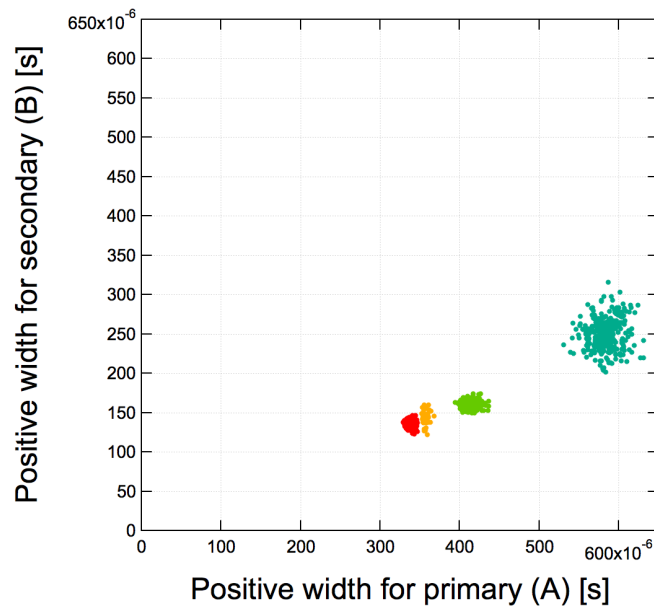


Figure 4.12: Peak width in the secondary, downstream channel vs width in the primary, upstream channel, from the 100618.02 measurement. Note that both axes have the same range. Widths are notably smaller in the secondary channel, suggesting a higher local speed here than in the primary channel, which in this case is ch.4. The dependence seems linear, and through (0,0). Each colour represents a peak class, each data point a peak.

A notable feature of figure 4.12 is the rather tight connection between the widths in the two channels, showing a dependence that might very well be linear and through (0,0), which could be due to the widths of all peaks changing by a constant factor between the channels, indicating a clamping-dependent effect.

It also shows that the larger variance in the secondary channel, seen in figures 4.13 and 4.14, is not necessarily a recurring feature.

⁵figure 4.14, from another experiment and at a different temperature, also fits into this.

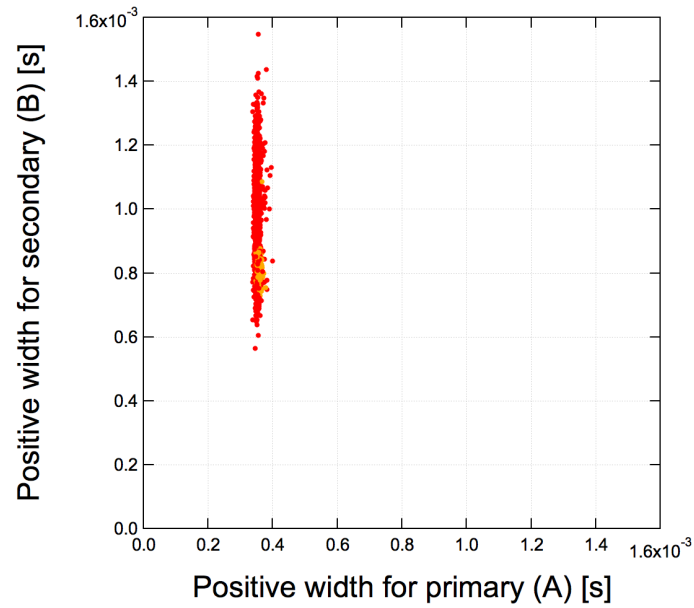


Figure 4.13: Peak widths in primary vs secondary channels, in the 100203_07 measurement. Widths are larger in the secondary channel, which here is downstream and is ch.4.

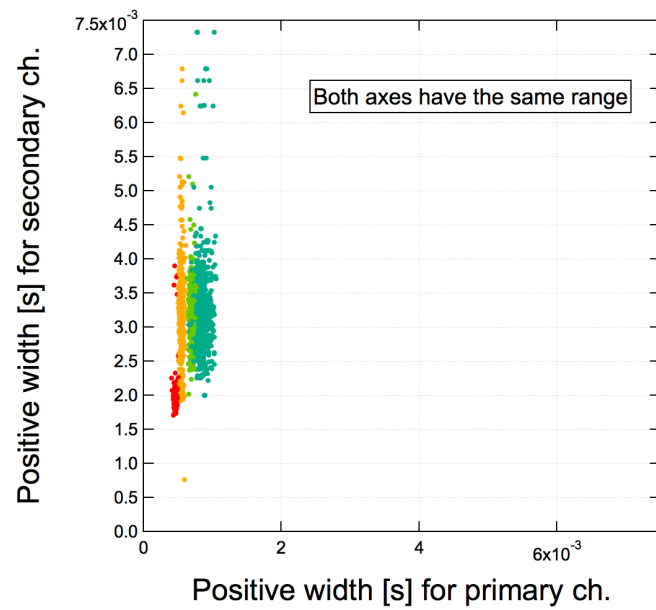


Figure 4.14: Peak widths in primary vs secondary channels, in the 101007_08 measurement. Widths are larger in the secondary channel, which here is downstream and is ch.4. The temperature is 6°C, as opposed to 15°C in figures 4.12 and 4.13.

4.4.2 Peak width, local speed and average speed

The term 'peak width' denotes the full width *in time* (unless otherwise noted, at half maximum and of the first positive phase) of an action potential signal. It is thus a measure of the time it takes the signal to pass the electrode that measures it.

It is not the *total* width of the signal (as it would be, if taken at the level of the baseline) and the value of the peak width is thus somewhat smaller than the total time of passage of the signal. But assuming that the overall shape of the peaks are similar, it should be a fairly good measure of the passage time.

The time it takes for the signal to pass the stretch of nerve that the electrode is measuring on (i.e. the part of the nerve that is clamped inside the electrode's glass capillary) of course depends on the length l_n of that nerve stretch. The longer the stretch, the longer it takes for the signal to pass it. But if l_n is small compared to the length l_s of the signal⁶, then the passage time is approximately proportional to the physical signal length l_s .

So, **assuming:**

- similarity of the overall shape of the peaks
- that the length l_n of the part of nerve being measured on is short, compared to the length l_s of the signal: $l_n \ll l_s$
- (and also, that the signal velocity is constant during passage of the electrode - that should hold though, since the length of the clamped part of nerve is on the order of maybe a few tenths of a mm, probably less)

then we get that the peak width in a specific channel becomes a fairly good measure of (i.e. \approx proportional to) the physical length of the action potential.

Furthermore, **assuming:**

1. that l_n is constant over the time course of a measurement (usually this was about 8-10 minutes) - i.e. that the clamping is stable, such that the nerve is not slipping into, or out of, the capillary
2. that the signal speed is constant between the two electrodes
3. that the distance d along the nerve between the two measuring electrodes is constant (this also follows from a stable clamping)

then

- following 1): the peak width is inversely proportional to the local speed v_{local} of the signal at the electrode
- following 2): v_{local} equals the average signal speed $v_{average}$ between electrodes
- following 3): there is a constant relationship between $v_{average}$ and the delay time t_{delay} between detecting the signal in the first electrode it passes, and detecting it in the second: $v_{average} = d/t_{delay}$

⁶the physical length (f.i. in mm)

Then the peak width should also be inversely proportional to $v_{average}$:

$$v_{average} = v_{local} \approx \frac{l_s}{w_{peak}} \quad (4.1)$$

where w_{peak} is the peak width.

If all assumptions hold, we thus have that

$$w_{peak} \propto v_{average}^{-1} \quad (4.2)$$

Is the signal speed constant?

We do not know for sure that the speed of a signal is constant when it runs along the nerve. According to Hodgkin's theoretical arguments in [3], the speed depends on the diameter of the neuronal fibre - speed being proportional to the square root of diameter (equation 2.5 in section 2.2. So if the neuron for instance has variable diameter along its length, then the speed should also vary accordingly.

Figure 4.6, middle panel, could be an inverse proportionality between width and speed, as would be the case if the speed was constant. But this does not in itself constitute a proof of constant speed. The same inverse proportionality would be the case, if all peak classes (the signals from all neurons in the nerve) would have the same speed change between the measuring electrodes, which would be the case if all neurons suffer the same relative diameter change between electrodes.

4.4.3 Peak-to-peak time

A further parameter related to the shape of the peaks is the peak-to-peak time (positive peak to negative peak), which is the time that elapses from the signal reaching its highest positive value to when it reaches its most negative value. Histograms of this parameter from two different measurements (100618_02 and 100203_10) are shown in figures 4.15 and 4.16. The temperature in both is 15°C (albeit on the way down in the temperature series in the 100618 data, and on the way up in the 100203 data). Note that one class from figure 4.15 is not present in figure 4.16. Therefore the class numberings are not exactly the same: classes A0, A1 and A3 in figure 4.15 correspond to A0, A1 and A2, respectively, in figure 4.16.

The average values and their standard deviations (Stdv) are as follows:

Peak-to-peak times in 100618_02		
Peak class	Average [ms]	Stdv [ms]
classA0	0.416	0.006
classA1	0.424	0.009
classA3	0.772	0.050
Peak-to-peak times in 100203_10		
Peak class	Average [ms]	Stdv [ms]
classA0	0.407	0.007
classA1	0.412	0.010
classA2	0.736	0.030

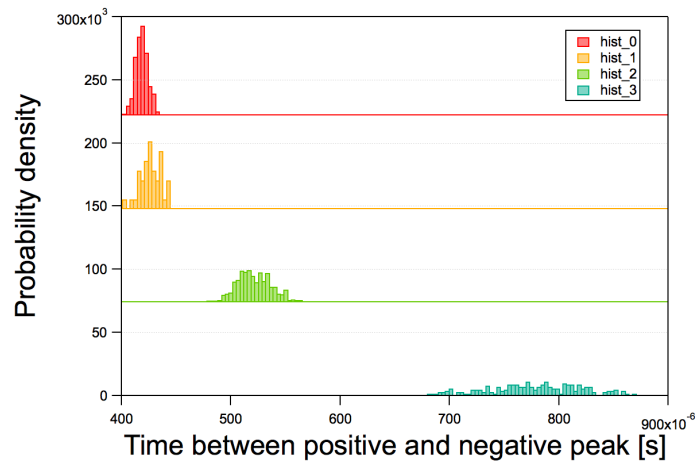


Figure 4.15: Histograms for positive peak to negative peak time difference, for the 100618.02 measurement. Compare with fig. 4.16 (in which the green class(A2) from this plot is not present).

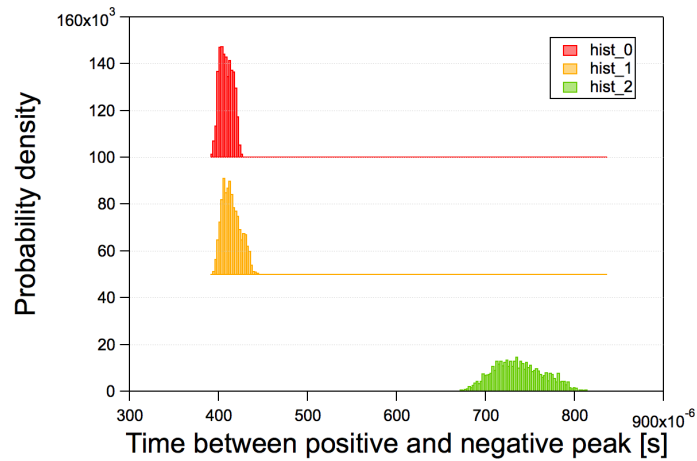


Figure 4.16: Peak-to-peak-time histograms for the 100203.10 measurement. Average values for the three classes are comparable to those for classes 0(red), 1(yellow) and 3(turquoise), respectively, in figure 4.15.

Peak-to-peak time is the same in both experiments, to within the sum of the classes' Stdv's. This goes for all three classes (recall that classA3 in the upper table is the same class as classA2 in the lower table).

The variation between classes within one measurement is probably due to differences in signal speed between the individual neurons, with slower speeds giving more stretched out signal shapes.

It is interesting though, that the peak-to-peak time for a given class seems to be quite stable between different experiments.

4.5 Inter-dependence of the parameters

Looking at figure 4.6 again, it is seen that the amplitudes, speeds and peak widths of the peak classes are correlated.

The upper panel shows a non-linear correlation between the positive amplitude and the average speed between the channels. The A0 and A1 classes in particular indicate that the amplitude tends to increase more rapidly at higher speeds.

Another plot of positive amplitude vs speed, previously presented in figure 4.5, shows an amplitude-speed correlation that - disregarding the two purple peaks at the top of the plot - looks more linear. It might also tend toward a slightly slower increasing amplitude with increasing speed.

The amplitude-speed correlation is only between peak classes - not *within* each class. That this is so makes sense, because both amplitude and speed depend on the axon diameter of the neuron associated with a peak class (see 2.2), and it is not likely that the axon diameter changes between the passing of each individual signal. Therefore all peaks in a given neuron should theoretically have the same amplitude and the same speed (the assumption of same amplitude being the prerequisite for classifying the peaks according to amplitude).

The variance of these two parameters within a class might then be attributed to background noise level and/or to the detection routine in the data processing software. For the amplitude, small variations in the clamping quality might also affect the detected amplitudes; we have already seen that measured amplitudes vary quite much between different experiments, which could be due to their dependence on the clamping quality.

Hodgkin on amplitude-speed relation

Recall from section 2.2 (equation 2.7) that according to [3] together with [5] $A \propto \theta^2$, where A is the amplitude and θ the signal speed.

If one instead adopts the view expected from theoretical grounds (according to Keynes and Aidley [5], p.19, first paragraph), that:

$$A \propto d^2 \tag{4.3}$$

where d is the nerve fibre diameter, then (together with equation 2.5) we find:

$$A \propto \theta \tag{4.4}$$

In either case, larger amplitude is correlated with larger speeds.

Here I have indications of both of these theoretical predictions for the amplitude-speed correlation. Figure 4.6 indicates an $A \propto \theta^2$ connection, while figure 4.5

might suggest $A \propto \theta$. (The two figures represent different experiments at different temperatures (15°C and 6°C, respectively), but that should not affect the correlation.)

Soliton model on amplitude-speed relation

According to the soliton model, pulses with larger amplitudes have smaller speeds, for a given neuron (thus for a given diameter) and for constant temperature. It must be noted that amplitude means something different in the soliton model than it does in the Hodgkin-Huxley model. In the former it is an amplitude in lateral density of the membrane, in the latter an amplitude of voltage - either between the inside and the outside of the membrane (for intracellular measurements), or between two positions outside the membrane (for extracellular measurements, like in this project).

How these two different amplitudes are connected, is not well known, but intuitively the most likely case seems to be that a large density-amplitude would also mean a large voltage-amplitude.

Assuming:

- that all signals, across all neurons in the nerve, is endowed with the same amount of energy when triggered
- that the different diameters of the individual neurons does not alter the parameters p and q (which quantify the non-linearity in $c^2(\rho^A)$, see figure 2.1) from equation 2.2 significantly

then we should be able to use the soliton model's amplitude-speed relation across different neurons (corresponding to different classes).

But in that case, the amplitude-speed data from figures 4.5 and 4.6 (upper panel) does not fit the soliton model. For this data to agree with the soliton model, we would have to have a negative correlation between the density-amplitude of the soliton model and the voltage-amplitude of the Hodgkin-Huxley model. This might initially be counter-intuitive, but as the connection has not yet been fully explored⁷, the possibility cannot be ruled out.

4.6 Temperature dependence of the parameters

Comparing average profiles of the peak classes from measurements made at different temperatures gives an indication of how the peak parameters change with temperature. Only the temperature was altered between the measurements, the clamping was left untouched. In the following the data from the 100203 experiment will be compared. This is a series of measurements conducted at temperatures 5°C apart, from 20°C down to 5° and then up to 30°. At different points drops of acetylcholine chloride (ACh) was dropped onto the nerve system in order to increase firing frequency to get more peaks and thus better statistics. The individual measurements are numbered 100203_XX, where XX is as follows:
05: 20°C
07: 15°C - ACh was added during the measurement

⁷although the topic is currently being investigated in the Membrane Biophysics Group at NBI.

08: 10°C
09: 5°C
(10°C on the way up is skipped because it has almost no signals)
10: 15°C
11: 20°C - a little ACh (one drop) was added
12: 25°C
13: 30°C

4.6.1 Identifying corresponding peak classes between measurements

The number of peak classes being detected varies between measurements and is not correlated with temperature. This is seen in figures 4.17 and 4.18, which both show the detected peak classes at 15°C, the first one on the way down in temperature, the second on the way up again. Comparing figures 4.18 (15°C)

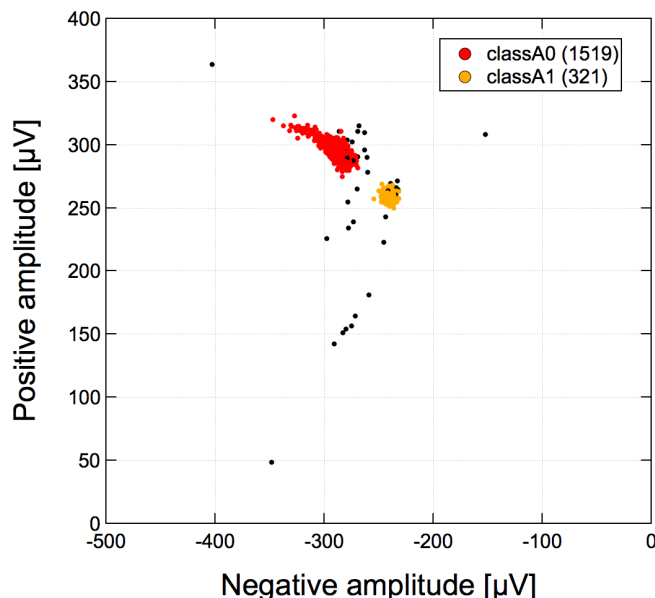


Figure 4.17: Positive vs negative amplitudes of peaks at 15°C, going DOWN in temperature (100203_07 measurement). Only two peak classes are detected. Amplitudes are in μV .

and 4.19 (10°C) it is apparent that it is not always easy to identify which classes correspond to each other across different measurements, due to changing amplitudes and number of peak classes.

The changing number of detected classes probably reflects a change in the number of active neurons. The higher number at the lower temperature (10°C) in figure 4.19 could have been explained by the soliton model's prediction that it is easier (demands less energy) to start a pulse when the temperature is lower, had it not been for the fact that there is no direct overall correlation between lower

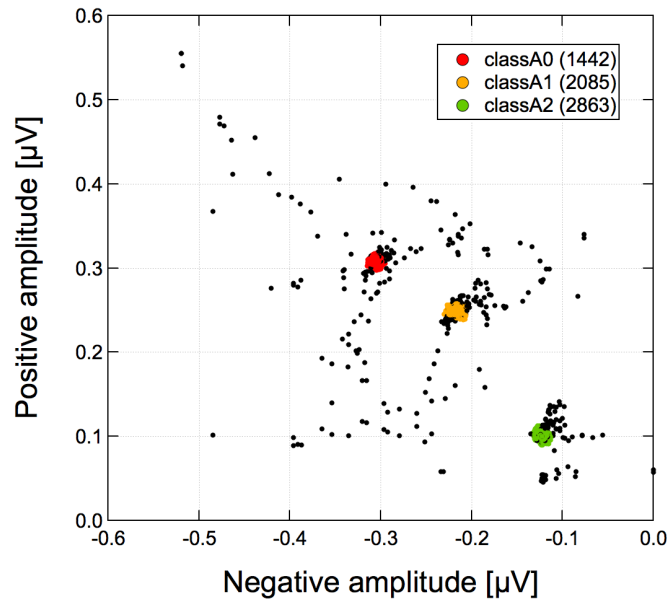


Figure 4.18: Positive vs negative amplitudes of peaks at 15°C, going UP in temperature (100203_10 measurement). Here three peak classes are detected. It is unclear which of these, if any, coincide with the two from fig. 4.17. Here amplitudes are in mV.

temperatures and higher numbers of peak classes detected. Instead there seems to be a better coherence in the number of classes in the measurements taken when increasing the temperature between each measurement, as compared to when decreasing it (see table below):

Number of detected peak classes	
Temperature	# of classes
20°C	2
15°C	2
10°C	5
5°C	2
15°C	3
20°C	3
25°C	3
30°C	3

It seems the number of detected classes fluctuates somewhat on the way down in temperature, but becomes stable once the temperature is rising again. This is probably not caused simply by the lowering of the temperature down to 5°C, since a drop to approximately the same temperature (most likely around 3 to 4°C) was used to anaesthetize the crayfish prior to the measurement.

At first glance, one might think that the yellow(A1), turquoise(A3) and blue(A4) classes in figure 4.19 are the same as the red(A0), yellow(A1) and green(A2)

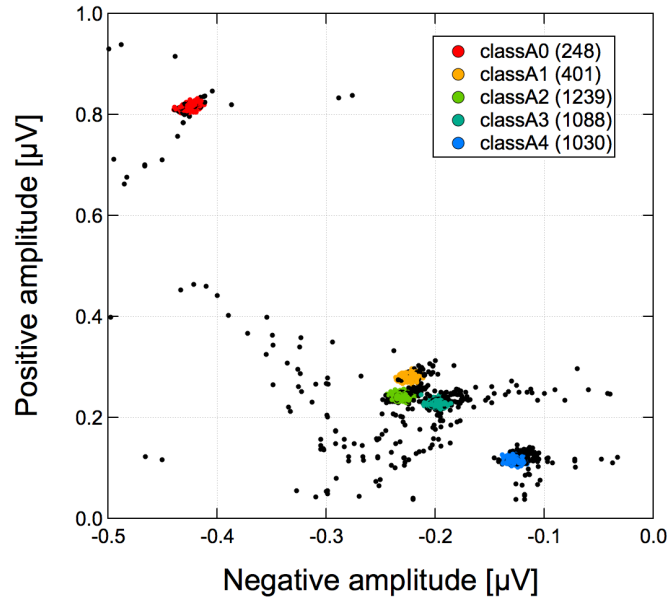


Figure 4.19: Positive vs negative amplitudes of peaks at 10°C , going down in temperature (100203_08 measurement). Five peak classes are detected (contrasting that, at 10°C on the way up, almost no signals were present). Amplitudes here in mV.

classes in figure 4.18. A closer look at the average values and standard deviations of both amplitude, width and peak-to-peak time, on the other hand shows that it is far more likely that the only two classes in the 10°C measurement (figure 4.19) that are also present at the other four temperatures of interest, are the green(A2) and the turquoise(A3). They correspond to the red(A0) and the yellow(A1), respectively, in figure 4.18. The three classes in the latter figure are also present at 20, 25 and 30°C , so I will be comparing parameters at these temperatures: 10, 15, 20, 25 and 30°C (all on the way up in temperature).

4.6.2 Comparing average peak profiles

The three figures 4.20, 4.21 and 4.22 show average peak profiles for the same three classes at different temperatures - 15°C , 20°C and 30°C , all on the way back up in temperature. Vertical and horizontal scales are the same, so the peak shapes can be compared directly between figures. Comparing the (first) positive phases of the profiles, it looks like - for all three classes - the amplitudes increase and the peak widths decrease when going from 15°C up to 20°C ; and in going from 20°C to 30°C the amplitudes stay the same and the widths decrease further.

Amplitudes vs temperature

To quantify these indications, the average values and standard deviations (Stdv) were calculated from Gauss curves fitted to histograms of the amplitude and

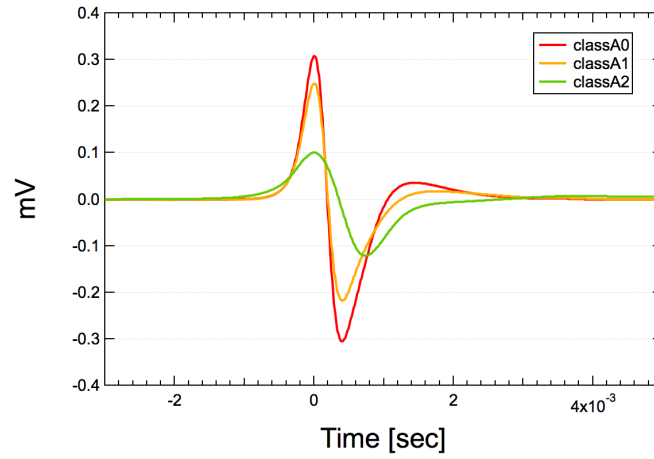


Figure 4.20: Peak profiles of the three classes at 15°C, each profile calculated as the average of all peaks in that class. Compare with figures 4.21 and 4.22.

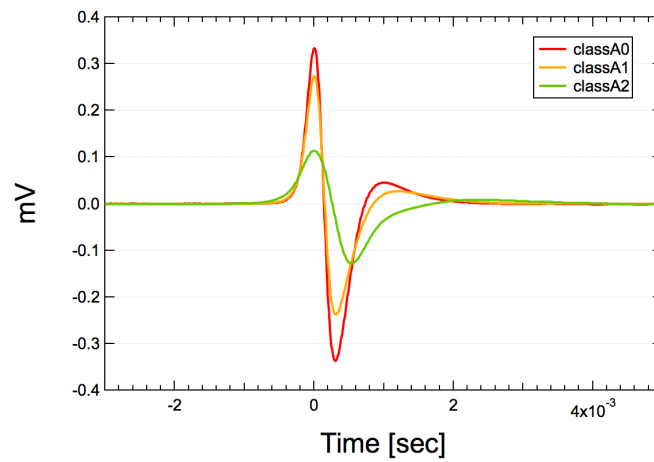


Figure 4.21: Average peak profiles of the three classes at 20°C. Compare with figures 4.20 and 4.22.

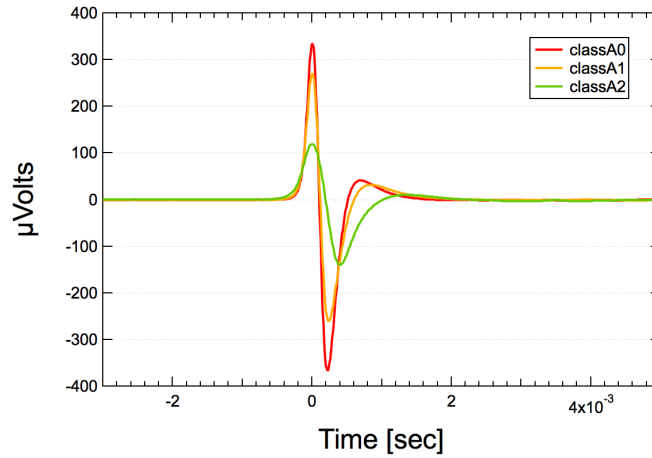


Figure 4.22: Average peak profiles at 30°C. Compare with figures 4.20 and 4.21.

width. This was done for each class and at each temperature. The results are seen below. (ClassA2 is lacking the 10°C data because the class is not detected at that temperature)

Amplitude of classA0

Temperature	Average [μV]	Stdv [μV]
10°C	241.948	3.795
15°C	308.196	3.057
20°C	333.942	3.307
25°C	343.836	3.383
30°C	335.197	3.221

Amplitude of classA1

Temperature	Average [μV]	Stdv [μV]
10°C	229.187	4.113
15°C	249.596	2.901
20°C	273.963	3.123
25°C	280.535	3.052
30°C	271.199	3.102

Amplitude of classA2

Temperature	Average [μV]	Stdv [μV]
15°C	100.732	3.165
20°C	114.051	3.172
25°C	123.669	2.925
30°C	119.867	3.227

Indeed, the amplitudes do increase at first, as suspected from the average peak profiles - but another interesting feature now shows up: It seems that somewhere between 25°C and 30°C, the amplitude begins to decrease again. The decrease is - at least for the A0 and A1 classes - statistically significant, in that it is larger than the sum of the standard deviations at the two temperatures.

The turnover in amplitude might instead be between 20°C and 25°C, but if it is between 25°C and 30°C, then it might have something to do with the fact that the stock of crayfish - up until the day of the experiment on them - were kept in an aquarium where the water temperature was approximately 27°C. This temperature naturally varied somewhat, but it was never below 25°C (at least not in the days up to an experiment) and never above 30°C.

Widths vs temperature

Data from Gauss curves fitted to the peak width histograms are seen below:

Width of classA0		
Temperature	Average [ms]	Stdv [ms]
10°C	0.361	0.006
15°C	0.312	0.007
20°C	0.220	0.002
25°C	0.184	0.003
30°C	0.154	0.003

Width of classA1		
Temperature	Average [ms]	Stdv [ms]
10°C	0.355	0.006
15°C	0.330	0.007
20°C	0.233	0.003
25°C	0.197	0.003
30°C	0.169	0.003

Width of classA2		
Temperature	Average [ms]	Stdv [ms]
15°C	0.584	0.025
20°C	0.390	0.012
25°C	0.339	0.011
30°C	0.273	0.008

First, a note on the standard deviation. It is seen that it has a tendency to decrease with higher temperatures. This is likely to be a side effect of the signals having narrower widths and larger amplitudes, at higher temperatures. The data processing routine calculates the peak width from those time values where it detects that the voltage has increased to half the maximum value of the pulse. The noise present in the data causes an uncertainty in these time values, and the magnitude of this uncertainty depends on how steep the voltage curve is at the critical time values.

The taller and narrower pulses at high temperatures have a more steep slope and thus their widths are detected with higher precision by the routine - resulting in smaller standard deviations. Such a temperature correlation is not seen for the amplitudes.

Secondly, the peak widths themselves. The numbers confirm what was suspected from the average peak profiles. The widths continually get smaller with increasing temperature, in all cases by more than what can be expected from the standard deviations.

This might simply be because their speeds increase (see speed tables below), and the signal lengths are constant - or it might be that the signals get shorter,

while their speed is constant. It could also instead be a combination of changing speeds and lengths. The data allows one constraint, though:

Assuming:

- that the width change is not caused by the measuring equipment

the possibility of signals becoming both slower and longer with increasing temperature, is excluded, since this would give larger peak widths.

The most obvious way the equipment could cause smaller widths, would be if the length of nerve clamped within the electrode capillary would continually become shorter. This would be the case if the suction clamping would lose strength such that the nerve would gradually slip out. Such a scenario can not be excluded.

4.6.3 Interpretation of amplitude and width results

Amplitude

The soliton model predicts that more energy is needed at higher temperatures than at lower ones, to generate pulses of the same density-amplitude.

Assuming

- that there is a more or less close correspondence between the voltage-amplitudes measured here, and the density-amplitudes
- that (at least for a given neuron) the nerve system puts the same amount of energy into each pulse, regardless of temperature

then we would have lower amplitudes at higher temperatures - the opposite of what the data says.

On the other hand, the turnover in amplitude somewhere above 20°C, in the data suggests that the nerve system does not always fire pulses with the same energy. Indeed it is not unthinkable that the second assumption above does not hold, and that the nerve system has more energy available at higher temperatures to put into each pulse.

Thus we could have a scenario with two opposing effects:

1. The energy given to each pulse, and with that its amplitude, might **increase** with temperature in some unknown way.
2. The resulting amplitude of a pulse, given a certain amount of energy, would - according to the soliton model - **decrease** with higher temperatures.

If the temperature dependence of these two effects is not the same - and there is no reason to believe that they should be - then we might have that the first one would dominate at lower temperatures, while the second then could assume domination above a certain critical temperature. This could explain the turn from rising to falling amplitudes with increasing temperatures.

Width

When it comes to the velocity of the pulse, the soliton model predicts the opposite of what it says about the amplitude: The resulting velocity of a pulse,

given a certain amount of energy, would *increase* with temperature.

If we want to explain the decreasing widths when the temperatures rise, in terms of increasing speeds - as are found for the average speed between channels (see below), we would conversely have to assume that the increase in energy given to each pulse, caused by the increasing temperature (effect no. 1, above), does *not* dominate anywhere in the considered temperature range (10°C to 30°C).

So if effect no. 2 above is not anywhere dominated by no. 1, then higher temperatures would in total result in pulses with lower energies, and thus - according to the soliton model - in higher velocities, and in turn smaller widths, in accordance with the data.

Thus, opposing assumptions would have to be made simultaneously in order to bring both the amplitude data and the width data in accordance with the soliton model's predictions.

Another possibility to explain the decreasing widths - which might solve this problem - is shorter pulses, although there is no direct evidence for this.

Speeds vs temperature

First note that the speed parameter is the only one of the four considered here (the others being amplitude, width and peak-to-peak time) that is based both on data from the primary channel as well as from the secondary channel. The other three are only based on primary channel data.

The average speeds, as calculated from the propagation time between channels, and their standard deviations (Stdv) were likewise calculated from Gauss curves fitted to histograms of the speeds. The results are:

Speed of classA0		
Temperature	Average [m/s]	Stdv [m/s]
10°C	1.050398	0.058179
15°C	1.150846	0.061561
20°C	1.505470	0.061041
25°C	1.684824	0.087128
30°C	1.857982	0.374751
Speed of classA1		
Temperature	Average [m/s]	Stdv [m/s]
10°C	1.054690	0.083376
15°C	0.924407	0.362164
20°C	1.416956	0.018155
25°C	1.616096	0.029428
30°C	1.837710	0.034578
Speed of classA2		
Temperature	Average [m/s]	Stdv [m/s]
15°C	0.620463	0.021270
20°C	0.835942	0.022897
25°C	0.943536	0.046089
30°C	1.089888	0.037061

The general trend is that speeds increase with temperature.

The speed histograms for 10°C are seen in figure 4.23. Note here that the

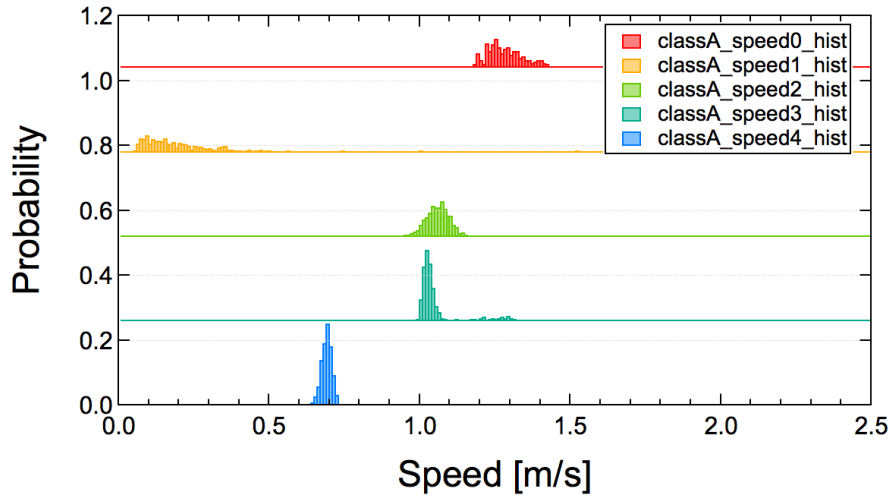


Figure 4.23: Speed histograms for the five peak classes present at 10°C (100203.08 measurement). Note that class numbering does not fit the speed tables. A0 and A1 in the tables are here A2 and A3, respectively. The remaining three classes do not correspond well to any of those at the other temperatures.

numbering of the classes does not correspond with the one in the speed tables. Classes A0 and A1 in the tables are A2 and A3 in figure 4.23, respectively. The figure shows a population with low speeds in the yellow class. These are due to the fact that at this temperature some of the peaks in that class were not detected in the secondary channel. As described in section 4.2, this leads to much smaller speeds.

The large Stdv at 30°C in classA0 is most likely also due to the lack of peak detection in the secondary channel mentioned above, but to a much lesser degree. The effect can be seen (the small bumps in the left part of the red trace) in figure 4.24, which shows the speed histograms for 30°C. The same effect is again at play in classA1 at 15°C, to an intermediate degree, affecting both average downwards and Stdv upwards.

4.6.4 Interpretation of speed results

The same arguments as for the smaller widths, when they are interpreted as higher speeds, can be used here, since the speeds increase with temperature. That is, as long as the amount of energy assigned by the nerve system to each pulse does not rise too quickly with temperature, then the soliton model's prediction of higher velocities for lower pulse energies can explain the speed data - since lower energies then would correspond to higher temperatures.

4.6.5 Peak-to-peak times vs temperature

Recall that the peak-to-peak time is the time elapsed between the pulse reaching its maximum positive value, and it reaching its maximum negative value.

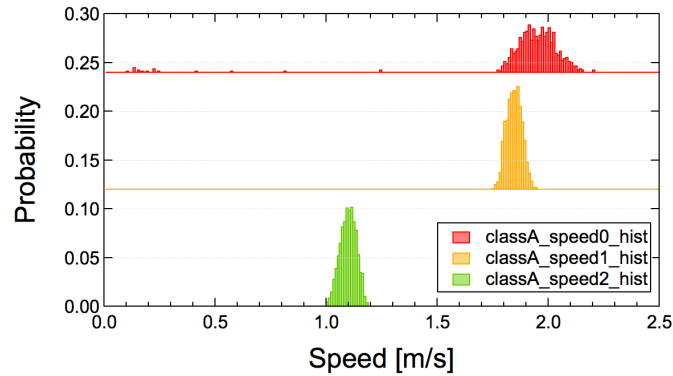


Figure 4.24: Speed histograms at 30°C (100203.13 measurement), showing a small number of peaks at low speeds in the red trace. These increase the standard deviation of the class.

Following the same procedure as for amplitude, width and speed above, the Gauss curves fitted to the peak-to-peak histograms give the following results:

Peak-to-peak time of classA0		
Temperature	Average [ms]	Stdv [ms]
10°C	0.452	0.006
15°C	0.407	0.007
20°C	0.311	0.002
25°C	0.264	0.004
30°C	0.228	0.003

Peak-to-peak time of classA1		
Temperature	Average [ms]	Stdv [ms]
10°C	0.427	0.006
15°C	0.412	0.010
20°C	0.319	0.003
25°C	0.277	0.004
30°C	0.246	0.003

Peak-to-peak time of classA2		
Temperature	Average [ms]	Stdv [ms]
15°C	0.736	0.030
20°C	0.540	0.014
25°C	0.469	0.012
30°C	0.404	0.009

In general, peak-to-peak times decrease the higher the temperature is, much like is the case for the peak widths.

Similar arguments for the interpretation apply, as for the peak widths.

4.6.6 Recap of temperature dependence

The temperature dependences of amplitude, width, speed and peak-to-peak time are shown in the figures 4.25, 4.26, 4.27 and 4.28. The figures are plots of the

data from the tables above.

Note that the amplitude increases up to 25°C, and then decreases above that. Note also the similarity of the curves for width, speed and peak-to-peak time. If signal speed and length are constant, then these three parameters are closely related. Within the plots for each of them the three peak classes have similar behaviour, especially the red and yellow ones, suggesting that the temperature has similar effects on the three neurons, which the classes represent. Between 15°C and 20°C there is a difference in the effect of the temperature on classA2 on one hand, and the classes A0 and A1 on the other. Temperature has a larger effect on both width and peak-to-peak time in classA2 than in the other two classes. In addition the temperature effect on the average speed (figure 4.27) is approximately the same, or possibly smaller, on classA2, compared to the other classes. This might be an indication of these three parameters not always being closely related, and thus that signal speed and length might not both be constant.

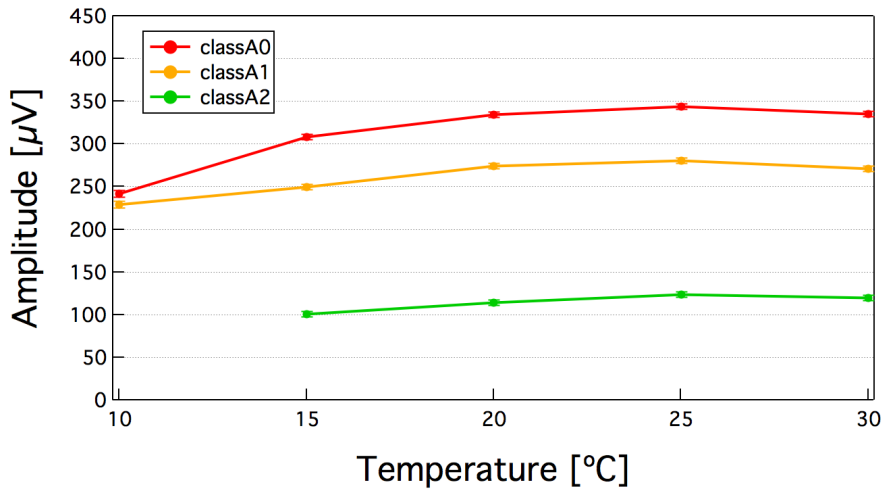


Figure 4.25: Amplitudes vs temperature for the three recurring classes in the 100203 experiment. Error bars are \pm one standard deviation. Note the decrease above 25°C.

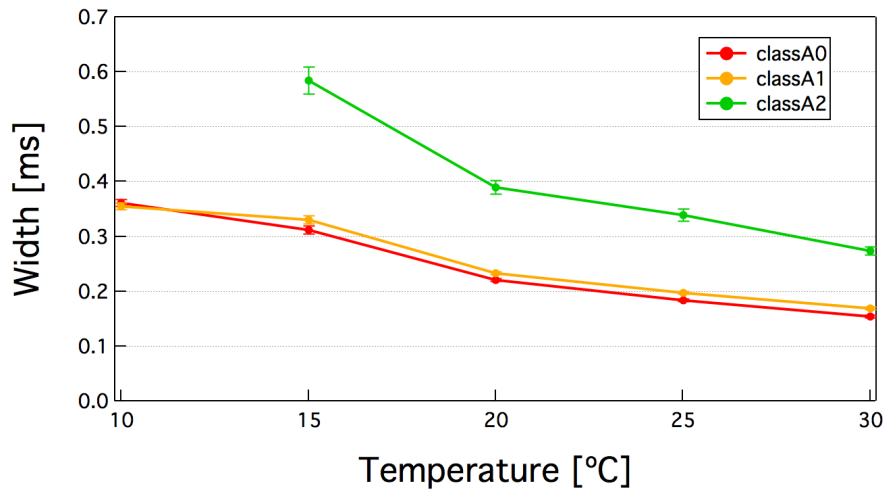


Figure 4.26: Peak widths vs temperature for the three recurring classes in the 100203 experiment. Error bars are \pm one standard deviation.

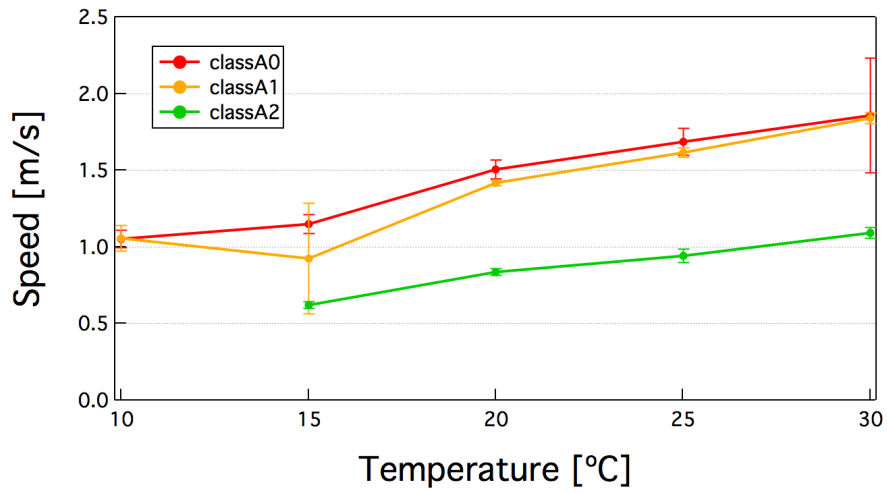


Figure 4.27: Speeds vs temperature for the three recurring classes in the 100203 experiment. Error bars are \pm one standard deviation.

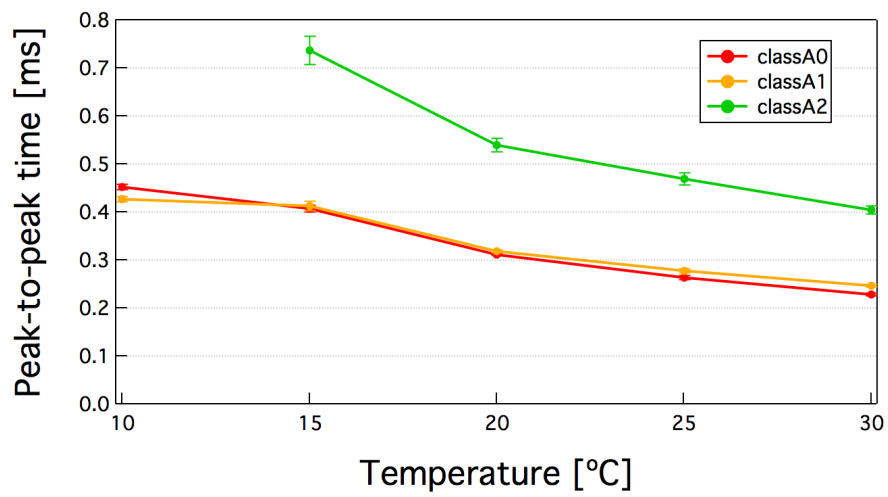


Figure 4.28: Peak-to-peak times vs temperature for the three recurring classes in the 100203 experiment. Error bars are \pm one standard deviation.

Chapter 5

Conclusions

The purpose of this project has been trying to take steps towards joining the electrical measurements of action potentials - which historically was the foundation for the currently accepted model for nerve signals: the Hodgkin-Huxley model - with the mechanically and thermodynamically founded soliton model. For this purpose I have electrically recorded the action potentials from a nerve, determined some of their characterizing parameters, and, where possible, compared those - especially their temperature dependence - with the predictions of the soliton model.

I have used two sets of differential electrodes to record the spontaneous action potentials from a motor nerve, containing six individual neurons, in the abdomen of specimens of the Australian red claw crayfish. The extracellular potential of the nerve was measured simultaneously at two different positions, a few mm apart, in order to be able to get measures of the signal speed.

These measurements were repeated at approximately regular temperature intervals in the range between 5°C and 30°C, thus producing a temperature series of data. Several such experiments were carried out at separate sessions on different days, and on different crayfish specimens.

Data was analysed using a data processing routine in Igor Pro, which detected corresponding peaks (= action potentials) in both data channels, with each channel corresponding to one of the electrodes. The routine detected and calculated amplitudes and peak widths (at half maximum) for both the first positive and the first negative phase of each pulse. It also calculated average signal speeds between the electrodes as well as peak-to-peak times (time between positive and negative extrema).

The detected peaks were classified manually according to their positive and negative amplitudes. Gauss curves were fitted to histograms of the four parameters mentioned above: the amplitudes, peak widths, speeds and peak-to-peak times. From these curve fits the average values and their standard deviations were found for each parameter.

The four pulse parameters were then analysed for variation between different experiments, for dependence on each other, and for temperature dependence. Relevant results were compared to the predictions of the soliton model.

The main results, in approximately the same order in which they occur in the text, are as follows:

1. The amplitude varies significantly between experiments, whereas the speed and width in the primary channel is comparably unchanged.
2. The width in the secondary channel varies considerably between experiments. This might be due to detection uncertainty caused by the lower signal-to-noise ratio in the secondary channel.
3. The amplitudes and peak shapes are not conserved from the upstream to the downstream channel. Nor is the order of the amplitudes of the peak classes.
4. The electrode designated as channel 4 consistently, across three different experiments (that is, on three different days) measured larger widths than the other electrode, regardless of upstream/downstream position. The explanation for this width discrepancy between electrodes is unclear, but it is of course most likely linked to the equipment, and not real. A linear correlation between widths in the two channels in one particular measurement, though, seems to suggest that all neurons are equally affected by it.
5. Generally better signal quality in the upstream channel than in downstream could be due to the upstream clamping affecting the neurons' ability to transmit the signals unchanged.
6. It can not readily be proven from the data that the signal speed is constant along the nerve.
7. There are indications from two different measurements that support two different amplitude-speed relations, both positive correlations: $A \propto \theta^2$ as well as $A \propto \theta$ are supported (where A is amplitude and θ is speed).
8. Positive correlation between amplitude and speed does not fit the soliton models predictions, if the following two assumptions hold: 1. that all signals, across all neurons in the nerve, is endowed with the same amount of energy when triggered. And 2. that the different diameters of the individual neurons does not significantly alter the parameters p and q (which quantify the non-linearity in $c^2(\rho^A)$).
9. There seems to be a kind of hysteresis in the number of detected peak classes, when going down in temperature between measurements as compared with when going up again. Going up the number of classes is stable, going down it is not. This is not an effect solely of moving the system down to around 5°C , since this was already done to anaesthetise the crayfish immediately before the experiment. It could be a short-term effect of it, though.
10. There is an indication that peak-to-peak times seems to be rather stable between experiments. This parameter might prove to be a more consistent measure of the signal length (and possibly of local speed) than the peak width.
11. Amplitude as a function of temperature has a maximum somewhere between 20°C and 30°C . This is, interestingly, consistent with the temperature in the aquarium in which the crayfish were kept prior to experiments.

12. Peak widths decrease with increasing temperature, giving the constraint that we cannot have that the signals become *both* slower *and* longer with increasing temperature - given that the width decrease is not caused by the equipment.
13. Amplitudes that increase with temperatures is not in accordance with the soliton model. But the fact that the amplitude begins to *decrease* above a certain temperature opens up the possibility of a scenario with two opposing effects: one that increases amplitude with temperature due to a rise with temperature in the amount of energy given to each pulse (caused by some as yet unknown mechanism); and another - predicted by the soliton model - that decreases the amplitude at higher temperatures. The first effect would then dominate *below* the critical temperature, where the amplitude has its maximum - whereas the second would dominate *above*.

Unfortunately, the same model cannot readily be used to explain that the widths decrease with increasing temperature - at least not if the width decrease is to be explained as an increase in speed. In that case one has to conversely assume that the latter effect mentioned above is not dominated by the other one anywhere in the considered temperature range (10°C to 30°C).

Both amplitude and width data might be in accordance with the soliton model, if another explanation of the width data were to be found; one that does not interpret the width solely as an inverse of the signal speed. This of course would be in effect, if the pulse length would decrease with increasing temperature, but there is no direct evidence for this.

14. There may be a vague indication at least, though - in the data for width, speed and peak-to-peak time as functions of temperature - that speed and length might not both be constant. So if this holds, and the speed is constant, then the temperature dependences of both amplitude and width data might still be in accordance with the soliton model.

The general picture that emerges is that the electrical measurements of action potentials I have made during this project - maybe not so surprisingly - does not immediately fit the soliton models predictions about the temperature dependence of the amplitudes and speeds.

Regarding the amplitude, there is of course the missing link from the voltage-amplitude measured here to the density-amplitude of the soliton model. This still leaves room - maybe not a real hope, but at least room - for the electrically measured data to be in accordance with the mechanically founded soliton model.

Bibliography

- [1] Joseph Erlanger and Herbert S. Gasser. *Electrical Signs of Nervous Activity*. University of Pennsylvania Press, 1937.
- [2] Thomas Heimburg and Andrew D. Jackson. On soliton propagation in biomembranes and nerves. *Proc. Natl. Acad. Sci.*, 102:9790–9795, 2005.
- [3] A. L. Hodgkin. A note on conduction velocity. *J. Physiol.*, 125:221–224, 1954.
- [4] A. L. Hodgkin and A. F. Huxley. A quantitative description of membrane current and its application to conduction and excitation in nerve. *J. Physiol.*, 117:500–544, 1952.
- [5] Richard D. Keynes and David J. Aidley. *Nerve and Muscle*. Cambridge University Press, 2001.
- [6] Benny Lautrup, Andrew D. Jackson, and Thomas Heimburg. The stability of solitons in biomembranes and nerves. *arXiv:physics*, (0510106), 2005.
- [7] S. Mitaku and T. Date. Anomalies of nanosecond ultrasonic relaxation in the lipid bilayer transition. *Biochimica et Biophysica Acta*, 688:411–421, 1982.
- [8] R. W. Murray. *Test Your Understanding of Neurophysiology*. Cambridge University Press, 1983.